AD-A142 846 A FLOW VISUALISATION STUDY TO TIP VORTEX FORMATION(U) 1/1
AERONAUTICAL RESEARCH LABS MELBOURNE (AUSTRALIA)
D H THOMPSON NOV 83 ARL/AERO-NOTE-421

UNCLASSIFIED F/G 20/4 NL

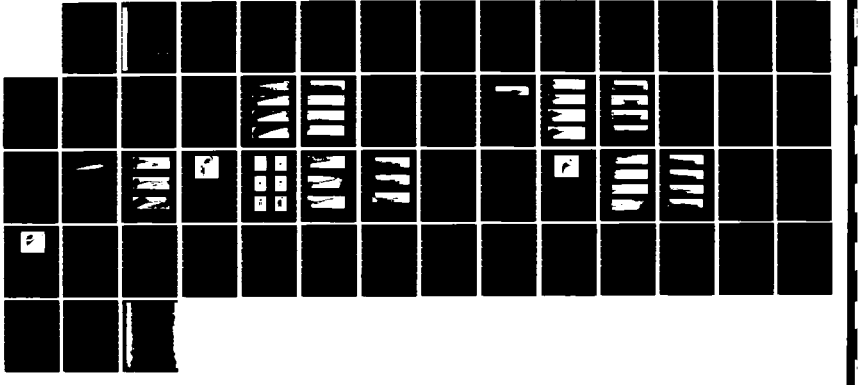

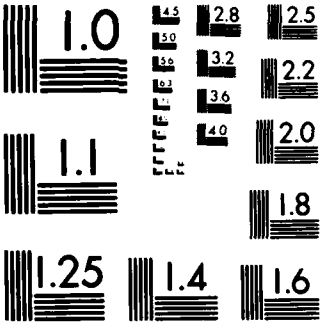

ARL-AERO-NOTE-421

AR-002-

DEPARTMENT OF DEFENCE

DEFENCE SCIENCE AND TECHNOLOGY ORGANISATION

AERONAUTICAL RESEARCH LABORATORIES

MELBOURNE, VICTORIA

AERODYNAMICS NOTE 421

A FLOW VISUALISATION STUDY OF TIP VORTEX FORMATION

by

D. H. Thompson

COPY No

NOVEMBER 1983

AR-002-988

DEPARTMENT OF DEFENCE
AERONAUTICAL RESEARCH LABORATORIES
DEFENCE SCIENCE AND TECHNOLOGY ORGANISATION

AERODYNAMICS NOTE 421

A FLOW VISUALISATION STUDY OF TIP VORTEX FORMATION

by

D. H. Thompson

SUMMARY

The process by which a wing or rotor blade tip vortex is generated has been studied in a water tunnel using dye and hydrogen bubble flow visualisation techniques. In particular, the effects of the shape of the lateral tip edge on vortex formation have been examined. Three edge shapes were tested—a square tip, a square tip with rounded fairing, and a square tip with bevelled fairing. The square tip was found to have the most complicated vortex system, with vortices forming on the tip edge face as well as above the wing. The observed flow features were generally similar to those proposed in the literature on the basis of pressure measurements, velocity measurements and surface flow visualisation in wind tunnels and on whirl towers. The vortex systems for the rounded and bevelled tips were less complicated. The shape of the tip edge has a significant effect on the structure of the tip vortex system, and may thus influence the tip loading characteristics. Verification of this would require further testing.

POSTAL ADDRESS: Director, Aeronautical Research Laboratories,
Box 4331, P.O., Melbourne, Victoria, 3001, Australia

CONTENTS

A FLOW VISUALISATION STUDY OF TIP VORTEX FORMATION

1. INTRODUCTION

At the tip of a lifting wing or rotor blade, flow separation occurs, leading to the formation of a vortex system above the rear upper tip surface. The resulting region of reduced pressure on the tip surface generates greater lift at the tip than would otherwise occur. The vortex also causes the centre of pressure to move aft, with a consequent increase in drag and nose-down pitching moment.[1] These effects are particularly important for helicopter rotor blades, the tips of which operate at high dynamic pressure. The situation is further complicated by the variation with blade azimuth angle of the vortex position over the blade tip, resulting in the application of fluctuating loads to the rotor control system.[1]

Tip vortices also play an important part in the generation of helicopter and fixed wing aircraft noise. The local separated flow at a rotor blade tip is a source of high frequency broad-band noise,[2] and the downstream interaction between a blade tip vortex and a following blade is a source of the blade slap component of helicopter noise.[3] The vortex flow round the side edges of flaps generates airframe noise from fixed wing aircraft,[4] and the interaction between a propeller blade tip vortex and the airframe of a propeller-driven aircraft is a source of cabin noise.[5] In marine applications, tip vortex flow is important in relation to the occurrence of cavitation at the tips of hydrofoils.[6]

Tip vortices are also significant with respect to flight safety, as the vortex wake trailed by an aircraft, particularly a large wide-bodied commercial aircraft, can pose a considerable hazard to following aircraft.[7]

Thus a detailed knowledge of the mechanisms by which vorticity is shed at, and transported round, the tip of a lifting blade or wing is important in many applications.

Wind tunnel studies of tip flows around fixed models have included the use of smoke,[8] helium bubble,[9] and surface flow[8,10] visualisation techniques, measurements of surface pressure distributions,[1,10,11] and mapping of the tip velocity field using hot wire anemometry.[9,11] In wind tunnel tests of complete rotor models, smoke[1] and surface flow[10,12] visualisation techniques have been used, tip surface pressure distributions have been measured,[13] and velocity fields mapped using laser Doppler velocimetry.[14] Surface flow[1] and smoke[15] visualisation techniques have also been used on full-scale rotors.

Limited tip surface pressure distributions have been measured on aircraft wings in flight.[16] Hoerner[17] has assembled some results on the effects of tip shape on the effective aspect ratio and induced drag of fixed wing aircraft.

Maskew[18] has developed a theoretical model of the tip vortex formation process, in which a knowledge of the position of the flow separation lines at the tip is important.

Surface pressure distributions and surface flow visualisation can provide only indirect information on possible flow patterns away from the surface. Smoke patterns can provide additional information, but not necessarily in fine detail. The use of hot-wire or laser Doppler anemometry to map a flowfield is time consuming and requires extensive instrumentation. As an alternative to the above techniques, flow visualisation in water provides a convenient method for studying tip flow patterns using simple equipment.

The object of the tests described here was to use flow visualisation techniques to examine the process of tip vortex formation at a square wing tip, and to study the effects of adding two simple fairings, one rounded and one bevelled, to the square tip. Earlier work[19] had indicated that the tip edge shape had a significant effect on the downstream development of the vortex. The majority of tests were conducted in a water tunnel using fluorescent dyes for flow visualisation. Some additional tests made use of the hydrogen bubble visualisation technique.

2. EXPERIMENTAL APPARATUS AND TECHNIQUES

2.1 Models

The wing model used for the tests consisted of two components—a basic wing mounted on a reflection plate on a turntable, and an interchangeable tip section. The outline shapes of the model components are shown in Fig. 1. The basic wing had a chord of 254 mm, a semispan of 76 mm, and a NACA 0012 section. With a tip fitted the complete model semispan was 127 mm. The wing and tips were made from fibreglass, with aluminium alloy ribs.

The square tip had a flat edge face, normal to the spanwise axis. The edge shape of the rounded tip was formed by rotation of the aerofoil section about its chord line. The bevelled tip had the same planform as the rounded tip, but its edge had a triangular cross-section, giving a lateral edge angle of 90°.

Three spanwise bulkheads divided each hollow tip into four compartments. The original intent was to supply dye to each compartment through a tube in the basic wing. It was hoped that this arrangement would allow the injection of dye at any point on the tip surface simply by drilling through the model skin into one or other of the internal compartments. However, initial tests showed that this system did not allow adequate control of the dye flow through individual holes, and so a system of individual dye tappings, each independently connected via its own control valve to the dye supply, was adopted. This system, although necessitating model disassembly to change dye hole positions, did provide satisfactory dye flow control.

2.2 Test Facilities

The water tunnel, which has been described in detail elsewhere,[20] has a vertical working section 250 mm square and 750 mm long through which water flows downwards. The complete wing model on its reflection plate was mounted on a turntable in the rear wall of the tunnel. The mounting system allowed incidence to be varied over a range of $\pm 20°$.

2.3 Experimental Techniques

For most of the water tunnel tests, fluorescein sodium dye was used for flow visualisation. Illumination was provided by pairs of 20 watt "black light" fluorescent tubes mounted on either side of, or in front of the working section, depending on particular photographic requirements. Dye was injected through appropriate tappings in the wing surface to suit the particular flow feature under investigation. The majority of photographs were either plan views or end views of the model. A limited number of crossflow plane photographs were taken using a sheet of light from a slide projector or, for later tests, from a 75 mW argon ion laser. The sheet of light was arranged to shine through the dye pattern in a plane normal to the freestream direction. The dye patterns in the crossflow plane were photographed by means of a mirror downstream of the model, at an angle of 45° to the flow direction.

For the square tip, a number of crossflow photographs were taken using the hydrogen bubble flow visualisation technique. For these tests a chordwise electrode of fine wire (0·075 mm dia.) was cemented to the undersurface of the wing, just inboard of the tip edge. The bubbles shed by this wire were entrained into the tip flow, and were illuminated by a sheet of light from the argon laser.

Photographs were taken on either FP4 (125 ASA) or HP5 (400 ASA) monochrome film using a Hasselblad 500 EL camera. A Wratten 2E filter was used to eliminate stray ultraviolet radiation from the blacklight tubes.

Flow patterns were photographed at incidence angles of 4°, 8°, 12° and 16°, and at a flow velocity of 100 mm/s, corresponding to a Reynolds number of 22 000 based on wing chord. Some additional photographs were taken at a velocity of 50 mm/s (Reynolds number = 11 000).

The positions of vortex cores and other flow features were measured from enlarged negative images and the results plotted graphically. The axes used for plotting the results are shown in Fig. 2. Each set of axes has its origin at the point of intersection of the wing leading edge and the chord line at the outboard end of the constant-section part of each model. The positive x direction

is aft along the chord line, the positive y direction is inboard along the leading edge, and the positive z direction is upwards normal to the chord line. Thus the positions of all flow features are plotted relative to the basic square tip, and the effects of adding fairings outboard of the x axis can be readily observed.

3. RESULTS AND DISCUSSION

3.1 Square Tip

The most prominent feature of the flow about the square tip is the vortex which forms above the rear part of the tip upper surface, just inboard of the tip edge. This vortex, which will be referred to as the main tip vortex, originates from a region on the forward upper surface of the tip and moves inboard and upwards as it moves towards the trailing edge. The vortex position varies with incidence, as shown in the sequence of photographs in Fig. 3(*a*) (side views) and Fig. 3(*b*) (plan views). The vortex positions are plotted in graphical form in Figs 4(*a*) and 4(*b*). (Note that the vertical scale has been enlarged for clarity.)

From the graphs for Fig. 4, it appears that the point of origin of the main tip vortex moves forward with increasing incidence, from approximately 35–40% chord at $\alpha = 4°$ to 10–15% chord at $\alpha = 16°$. Fluid entering the main tip vortex core from the wing lower surface reaches the core partly across the forward region of the tip edge face and partly round the outboard part of the leading edge. Ahead of the point of origin of the tip vortex, the flow on the upper surface close to the tip edge is moving inboard. Downstream of the vortex origin the surface flow turns outboard, under the influence of the vortex.

At $\alpha = 4°$, the main tip vortex core remains fairly straight back to the vicinity of the trailing edge, where it curves slightly to align with the freestream. With increasing incidence, the core develops kinks towards the trailing edge of the wing. The point at which the kinks begin to form moves forward with increasing incidence and at $\alpha = 16°$ has reached approximately the 70% chord position (Fig. 3(*a*)).

On the wing upper surface beneath the main tip vortex, the flow direction is outboard and aft until a point is reached where secondary separation occurs. The wing upper surface boundary layer separates and rolls up to form a small secondary vortex rotating in the opposite direction to the main tip vortex. This upper surface secondary vortex is visible in Fig. 5 ($\alpha = 16°$), just inboard of the tip edge. At about the 60% chord point, the dye trace of the core of the secondary vortex appears to be deflected outboard, leaves the surface, and becomes indistinct as it is entrained in the general tip vortex system.

The kinks which develop in the main tip vortex core towards the trailing edge appear to be caused by an interaction with another vortex, of the same sense, which has its origin on the lower forward part of the tip edge face. This vortex will be referred to as the first tip face vortex. The variation of its position with incidence is shown in the sequences of photographs in Fig. 6(*a*) (side views) and Fig. 6(*b*) (plan views), and graphically in Fig. 7. It can be seen that the vortex moves upwards as it moves aft along the tip face. As it rises above the level of the wing upper surface the vortex moves rapidly inboard and begins to interact with the main tip vortex, causing the kinks in the latter which were discussed above. The interaction of the two vortices is shown graphically in Fig. 8. As the first tip face vortex rolls round the main tip vortex, the core of the former becomes less clearly defined.

The first tip face vortex induces a flow downwards and aft on the tip face, as shown in Fig. 9. This flow separates to form a small secondary vortex rotating in the opposite direction to the first tip face vortex. Towards the trailing edge, the secondary vortex leaves the upper edge of the tip face and is entrained in the general tip vortex flow.

At higher angles of incidence, another tip face vortex is present. This is of the same sense as the first tip face vortex and is positioned below it, as shown in the photographs in Fig. 10. Fig. 10 also shows how the position of the second tip face vortex varies with incidence, and how it interacts with the first tip face vortex.

Fig. 11(*a*) shows a cross-section of the flow around the square tip at an incidence of 12 and at the 50% chord position. Most of the features discussed above can be identified in this photograph, made using dyes for flow visualisation.

Additional cross-flow photographs of the first and second tip face vortices were taken using the hydrogen bubble visualisation technique. The results are shown in Fig. 11(*b*), indicating how the positions of the two vortices change with downstream distance.

It will be noted in Figs 6(*b*), 7(*b*) and 11(*b*) that for $\alpha = 16°$, the first tip face vortex "rolls over" from the tip face on to the tip upper surface at $x/c \simeq 0{\cdot}6$. It is at this point that the upper surface secondary vortex visible in Fig. 5 and discussed above begins to move outboard. This movement is probably caused by the presence of the tip face vortex close to the wing upper surface.

It is apparent that the flow in the vicinity of a square tip, at least for the Reynolds number range of the present tests, is quite complicated. The tip vortex system just downstream of the trailing edge is in fact made up of a combination of the main tip vortex and the two tip face vortices (all of the same sense), and at least two small secondary vortices of the opposite sense.

3.2 Round Tip

As with the square tip, the most prominent feature of the flow over the round tip is the main tip vortex which forms above the rear part of the tip upper surface. The point of origin of the vortex lies on the forward upper surface of the tip, but is less clearly defined than is the case with the square tip. The variation with incidence of the main tip vortex position is shown in the photographs of Fig. 12(*a*) and 12(*b*) and graphically in Fig. 13(*a*) and 13(*b*). The trend of the variation in vortex position with incidence is similar to that for the square tip. However, the vortex core is less well defined by the injected dye, particularly at lower angles of incidence, and at $\alpha = 4°$ it was not possible to estimate the vortex position with sufficient accuracy to include in Fig. 13.

The kinks in the main tip vortex which develop towards the trailing edge are less pronounced than is the case with the square tip. This is attributed to the absence of tip face vortices. Beneath the main tip vortex, the surface flow direction is outboard and aft until separation occurs. The separated flow rolls up to form a secondary vortex of opposite sense to the main tip vortex. The secondary vortex is visible in the photographs in Fig. 12(*a*), for $\alpha = 12°$ and $16°$. Towards the trailing edge the secondary vortex leaves the surface and is entrained in the general tip vortex system.

There is some indication that there is a third vortex outboard of and below the main tip vortex, and rotating in the same direction. It proved difficult to inject dye into the third vortex alone. However, crossflow photographs with dye injected through all available surface tappings (Fig. 14) did show the third vortex in addition to the other vortices discussed above.

3.3 Bevelled Tip

This tip, with primary separation occurring at the lateral edge, produces a clearly defined main tip vortex core. The main tip vortex originates at the tip edge, near the wing leading edge. The vortex remains close to the tip edge, then gradually rises and moves inboard slightly as the trailing edge is approached. The position of the vortex and its variation with incidence is shown in the sequence of photographs in Fig. 15(*a*) and Fig. 15(*b*) and graphically in Fig. 16(*a*) and Fig. 16(*b*).

In side view, the main tip vortex lies below the level of the wing upper surface until the 70% chord position for $\alpha = 4°$, or the 40% chord position for $\alpha = 16°$.

As with the other tip shapes, the main tip vortex induces a surface flow beneath it. The surface flow moves outboard and downstream until separation occurs and a secondary vortex forms. The secondary vortex leaves the surface towards the trailing edge and enters the trailing vortex system.

There appears to be another vortex, of the same sense as the main tip vortex, and positioned outboard of it. Again it proved difficult to inject dye directly into this vortex, but it appears in the crossflow photograph in Fig. 17.

3.4 Comparison of Vortex Patterns for Different Tip Shapes

The positions of the main tip vortices for the three tip edge shapes are compared in Figs 18 and 19. In general, at a given angle of incidence, the vortex from the bevelled tip is positioned outboard of the vortex from the rounded tip. Both these vortices in turn are positioned further outboard than the vortex from the square tip.

With respect to their displacement from the wing chord plane, the vortices from the square and rounded tips follow roughly similar paths, at a given angle of incidence. The tip vortex from the bevelled tip, however, lies closer to the wing chord plane over the forward part of the tip, and further away from the wing chord plane over the aft part of the tip than do the vortices from the other tips. In addition, the point of origin of the bevelled tip vortex lies much further forward than is the case for the other tip shapes.

The vortex positions for the three tip shapes are compared in another way in Fig. 20. The variation with incidence of the vortex positions at each of a number of chordwise stations is shown. The diagrams show that both fairings displace the tip vortex outboard relative to its position above the square tip. For $x/c \leqslant 0{\cdot}6$, the bevelled fairing has the greatest effect on the tip vortex position, displacing it further outboard than does the rounded fairing. Also, for angles of incidence of 8° or less, the vortex from the bevelled fairing lies closer to the chord plane than is the case with the other two tips.

For $x/c > 0{\cdot}6$ the lateral positions of the bevelled fairing vortex lie quite close to those for the rounded fairing vortex, but are generally further from the chord plane at any particular incidence.

It appears that the addition of either the bevelled or rounded fairing to the square tip modifies the flow round the tip to a considerable extent, and that the effects of each fairing are different. It is likely that the vortex position changes caused by the fairings will modify the tip pressure distribution and thus the tip loads and moments. However, an accurate determination of these effects would require detailed pressure and/or velocity measurements in a wind tunnel.

3.5 Effect of Reynolds Number

A small number of photographs were taken at a flow velocity of 0·05 m/s. There appeared to be no significant difference between the vortex positions at this velocity and those at a velocity of 0·1 m/s. This is to be expected, since any major changes are likely to occur with increasing rather than decreasing Reynolds number, at the point where some parts of the boundary layer in the tip region become turbulent and the position of the separation lines is affected. The effects of Reynolds number are likely to be most significant for the round tip, as the square and faired tips have salient edges which fix at least the primary separation lines.

3.6 Comparison with Other Results

The downstream development of tip vortices has been studied extensively,[7] but only a limited number of results of detailed experiments on the formation of a tip vortex over the wing itself have been published. These experiments fall into three main categories:

(*a*) surface pressure measurements,

(*b*) surface flow visualisation, and

(*c*) velocity field measurements using hot wire or laser anemometry.

There have also been some flow visualisation studies using smoke and helium bubbles as tracers. Most of the studies have been concerned with square tips.

Surface flow visualisation near the tip of square-edged wing tips by Spivey,[1] Spivey and Moorhouse,[10] and Piziali and Trenka[8] show outflow on the rear part of the upper surface near the tip edge. This outflow is taken as an indication of the presence of a vortex above the wing.

Spivey[1] also mentions the possibility of a secondary vortex, of opposite sense, beneath and outboard of the main tip vortex. These interpretations of the surface flow patterns were supported by measured pressure distributions and generally agree with the vortex patterns observed in the present tests. However, a suction peak outboard of the main tip vortex which Spivey[1]

attributes to the upper surface secondary vortex possibly could be due to the tip face vortex or vortices moving inboard over the tip upper surface. As discussed in Para 3.1, the tip face vortex appears to entrain the upper surface secondary vortex into the general interacting vortex system.

Reference 12 reports the use of an ammonia diazonium salt surface flow visualisation technique to study the flow round a square-edged tip on a model rotor. Ammonia gas was injected through holes on the upper surface and edge face of the tip. The tip was coated with a diazonium salt solution and the reaction between the ammonia and the surface coating left dark traces indicating the local flow direction. At an incidence of 10°, the upper surface flow at the tip was observed to be in an inboard direction over the forward part of the tip, and outboard over the rear part of the tip, behaviour similar to that observed in the present tests and consistent with the presence of a tip vortex over the rear part of the tip. The pattern on the tip edge face indicated an upward flow over the forward part of the face, downward flow over the middle part of the face, and upward flow over the rear part of the face. These patterns indicate the presence on the tip face of a vortex of the same sense as the main tip vortex, as observed in the present water tunnel tests.

Reference 13 gives pressure distributions measured on the upper and lower surfaces of the square-edged tip of a rotor blade with a NACA 0012 section. The distributions are generally similar to those of Refs 1, 10 and 11. The scope of the tests was extended by adding a rounded fairing to the square tip. No pressure tappings were placed on the fairing itself, but the pressure measurements made on the main part of the tip indicate that the addition of the fairing moved the tip vortex outboard relative to its position on the unfaired tip. A similar outward displacement of the vortex was noted in the present tests.

Ref. 11 gives the results of hot wire anemometer measurements of the velocity field above a square-edged tip of NACA 0015 section at an incidence of 12°. The results show a typical vortex velocity profile over the rear part of the tip upper surface. In addition, in measurement planes at 75% chord and at the trailing edge, another vortex was detected, outboard of the main tip vortex and rotating in the same direction. In the light of the water tunnel results described here, this second outboard vortex could be explained as a tip face vortex, beginning to interact with the main tip vortex.

Francis and Kennedy[9] used hot wire anemometry to measure the velocity field round a NACA 64009 section wing with a square tip, at an angle of incidence of 4°. The projection of streamlines in the crossflow plane at 60% chord indicate the presence of a vortex above the tip upper surface, and a second vortex, of the same sense, on the tip edge face.

In an attempt to make quantitative comparisons of vortex trajectories between published wind tunnel results and the results of the water tunnel tests described here, two points should be borne in mind. Firstly, the Reynolds number of the water tunnel tests is generally at least one order of magnitude less than that of typical wind tunnel or rotor tower tests. All the boundary layers are laminar, with consequent effects on the position of separation lines (except where these are fixed at salient edges.) Secondly, the water tunnel model is large relative to the working section, and wall constraint effects will be considerable. No attempt has been made to accurately assess these effects, but a rough estimate indicates that the effective angle of incidence of the model could be 1–1·5° greater than the geometric incidence, at a geometric incidence of 12°.

With these considerations in mind, the position of the main tip vortex above a square tip as determined from the water tunnel tests, is compared in Fig. 21 with the positions of upper surface pressure minima from Refs 11 and 13. The agreement is reasonably good, with the wind tunnel results falling between the water tunnel results for $\alpha = 8°$ and $\alpha = 12°$, at least back to the 80% chord point. Beyond that point, the trace of the main tip vortex is deflected as it begins to interact with the tip face vortices. The surface pressure distributions would not show the details of such interactions, but would indicate the pressure field due to the merged vortices.

No comparison between the water tunnel results and the pressure measurements for a round tip in Ref. 13 can be made, as the available pressure distributions are not sufficiently detailed to allow the determination of the position of pressure minima.

To the knowledge of the present writer, the tip shape referred to in this Note as the bevelled tip, has been the subject of only one previous series of experiments,[16] in which such a tip was flight tested on the upper wing of a biplane. Chordwise pressure distributions on the Clark Y section wing were measured at a number of spanwise stations. The results indicated that "the

principle effect of the faired [bevelled] end on the square tip was to reduce greatly the load near the extreme tip at high values of wing C_N." There was also a slight decrease in nose-down pitching moment at low values of C_N. The chordwise pressure measuring station closest to the square tip was at $y/c = 0{\cdot}097$ (using the co-ordinate system of this Note), and thus details of the tip loading outboard of this station were not obtained. The effect of adding a fairing to the square tip would be to shift the tip vortex outboard, resulting in a reduced loading at the measuring station. However, the loading further outboard could be increased and would not have been recorded in the results on which the conclusions quoted above are based. The present water tunnel tests have indicated that the addition of a bevelled fairing does modify considerably the flow round a square tip, and so could affect the tip loading, but the determination of any such effects would require detailed measurements of pressure and velocity in the tip region.

4. CONCLUSIONS

This water tunnel study has shown that the structure of the tip vortex system in the immediate vicinity of a wing tip or rotor blade tip is significantly affected by the shape of the lateral edge of the tip. Of the three edge shapes tested—square tip, square tip with rounded fairing, and square tip with bevelled fairing—the square tip had the most complicated flow pattern, with several vortices forming on the tip edge face as well as above the tip. The addition of a rounded or bevelled fairing resulted in a simpler vortex system, displaced outboard relative to the square tip vortex system. In comparison with the square and rounded tips, the point of origin of the main tip vortex from the bevelled tip occurred further forward on the wing, and the distance of the vortex above the wing chord plane varied more rapidly with chordwise distance.

For the square tip, there is reasonable correlation between the flow features observed in the water tunnel and those described in the literature on the results of wind tunnel and whirl tower tests. The water tunnel tests, in most cases, provide confirmation or explanation of flow features inferred from pressure distributions, surface flow visualisation or hot wire anemometry in the wind tunnel and whirl tower tests. The quantitative agreement on measured vortex positions is also reasonably good, considering the wide variations in Reynolds number and other test conditions.

No detailed comparisons for rounded or bevelled tips were possible due to the lack of published test results. It is possible that the tip loading characteristics reported in flight tests of a bevelled tip could be explained by the changes to the structure of the tip vortex caused by this tip shape, but verification of this would require the measurement of detailed tip pressure distributions in a wind tunnel.

REFERENCES

1. Spivey, R. F. — Blade tip aerodynamics – profile and planform effects. American Helicopter Society, 24th Annual National Forum, May 1968, Paper 205.

2. George, A. R., Najjar, F. E., and Kim, Y. N. — Noise due to tip vortex formation on lifting rotors. AIAA 6th Aeroacoustics Conference, June 1980, Paper 80-1010.

3. Widnall, S. E., and Wolf, T. S. — Effect of tip vortex structure on helicopter noise due to blade-vortex interaction. J. of Aircraft, vol. 17, No. 10, October 1980, pp. 705-711.

4. Hardin, J. C. — Noise radiation from the side edges of flaps. AIAA J., vol. 18, No. 5, May 1980, pp. 549-552.

5. Millar, B. A., Dittmar, J. H., and Jeracki, R. J. — The propeller tip vortex – a possible contributor to aircraft cabin noise. NASA TM-81768, April 1981.

6. Souders, W. G., and Platzer, G. P. — Tip corvex cavitation characteristics and delay of inception on a three-dimensional hydrofoil. David Taylor Naval Ship Research and Development Center, Report No. DTNSRDC-81/007, April 1981.

7. ——— — Wake vortex minimisation: A symposium held in Washington, D.C., 25-26 February, 1976.

8. Piziali, R., and Trenka, A. — An experimental study of blade tip vortices. NASA CR 66860, January, 1970.

9. Francis, M. S., and Kennedy, D. A. — Formation of a trailing vortex. J. of Aircraft, vol. 16, No. 3, March 1979, pp. 148-154.

10. Spivey, W. A., and Moorhouse, G. G. — New insights into the design of swept-tip rotor blades. American Helicopter Society, 26th Annual National Forum, June, 1970, Preprint 420.

11. Chigier, N. A., and Corsiglia, V. R. — Tip vortices: velocity distributions. NASA TM-X-62087, September 1971.

12. Velkoff, H. R., Blaser, D. A., and Hoffman, J. D. — Investigations of boundary layers and tip flows of helicopter rotor blades. US AAMRDL-TR-71-73, May 1972.

13. Gray, R. B., McMahon, H. M., Shenoy, K. R., and Hammer, M. L. — Surface pressure measurements at two tips of a model helicopter rotor in hover. NASA CR 3281, 1980.

14. Ballard, J. D., Orloff, K. L., and Luebs, A. B. — Effect of tip planform on blade loading characteristics for a two-bladed rotor in hover. NASA TM-78615, 1979.

15. Mantay, W. R., Shidler, P. A., and Campbell, R. L. — Some results of the testing of a full-scale ogee-tip rotor. J. of Aircraft, vol. 16, No. 3, March 1979, pp. 215–221.

16. Rhode, R. V. — The influence of tip shape on the wing load distribution as determined by flight tests. NACA TR-500, 1934.

17. Hoerner, S. F. — Fluid Dynamic Drag. Hoerner Fluid Dynamics, 1965.

18. Maskew, B. — *Influence of rotor blade tip shape on tip vortex shedding—an unsteady, inviscid analysis.* American Helicopter Society, 36th Annual National Forum, May 1980, Preprint 80–6.

19. Thompson, D. H. — Experimental study of axial flow in wing-tip vortices. J. of Airctaft, vol. 12, No. 11, November 1975, pp. 910–911.

20. Thompson, D. H. — The use of dyes for water tunnel flow visualisation. ARL Aerodynamics Note 339, February 1973.

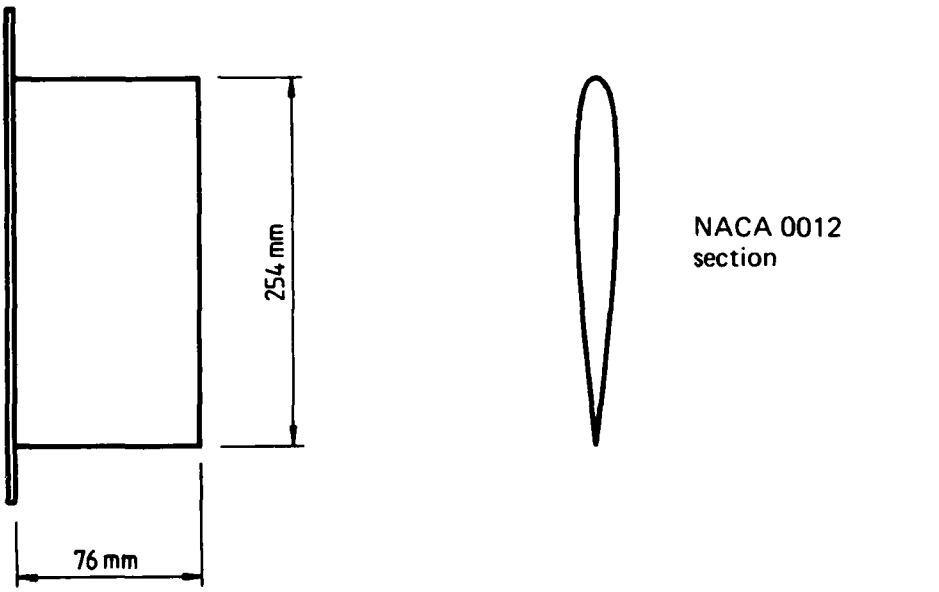

(a) Basic wing

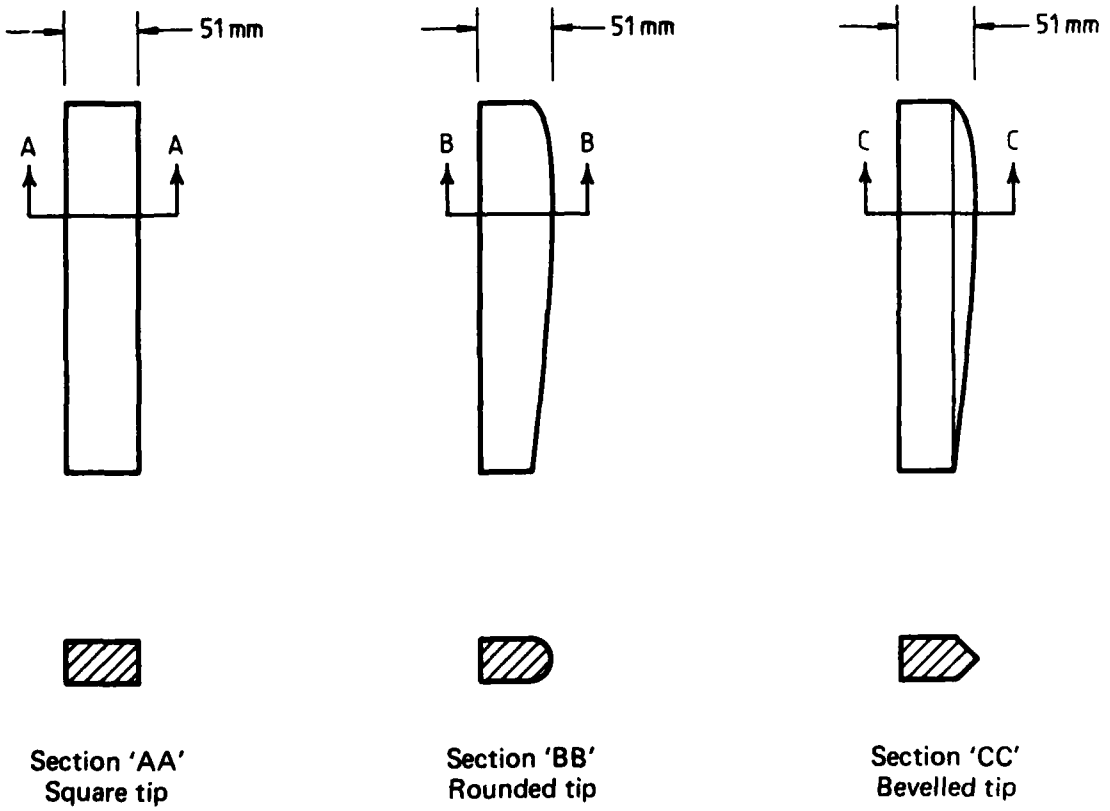

(b) Interchangeable tips

FIG. 1 WATER TUNNEL MODEL OUTLINES.

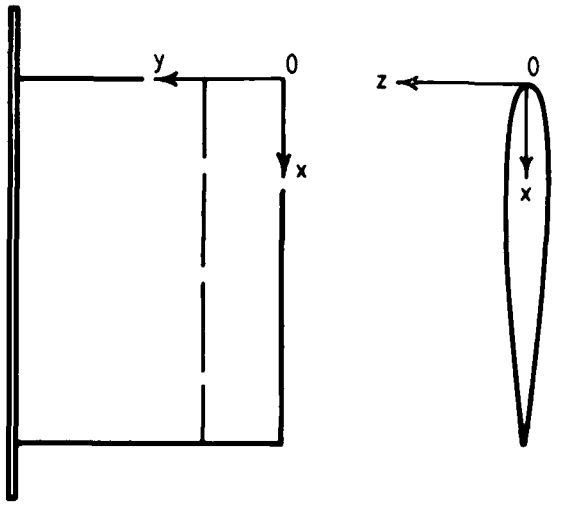

Square tip

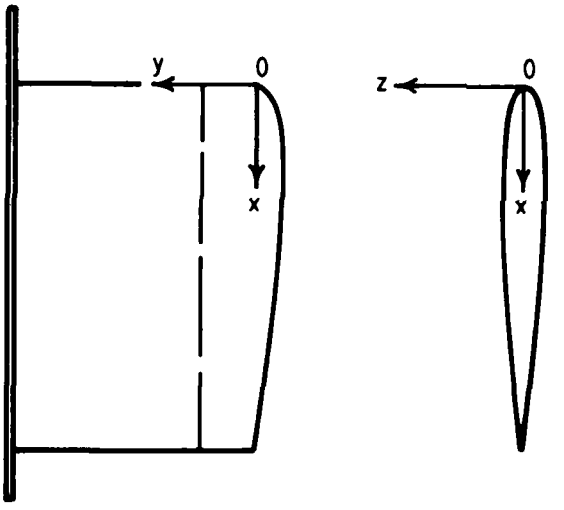

Rounded tip

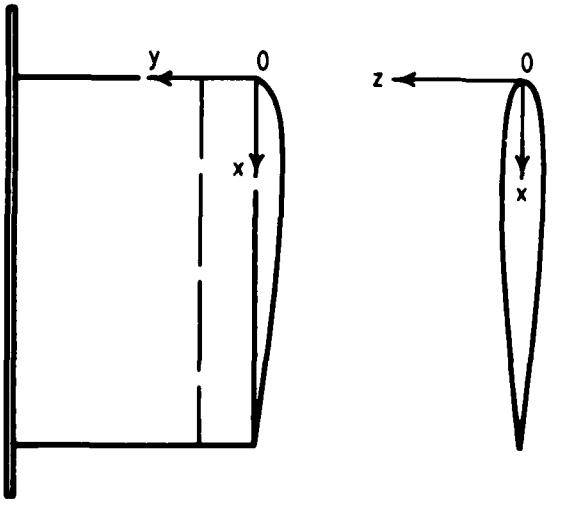

Bevelled tip

FIG. 2 MODEL REFERENCE AXES.

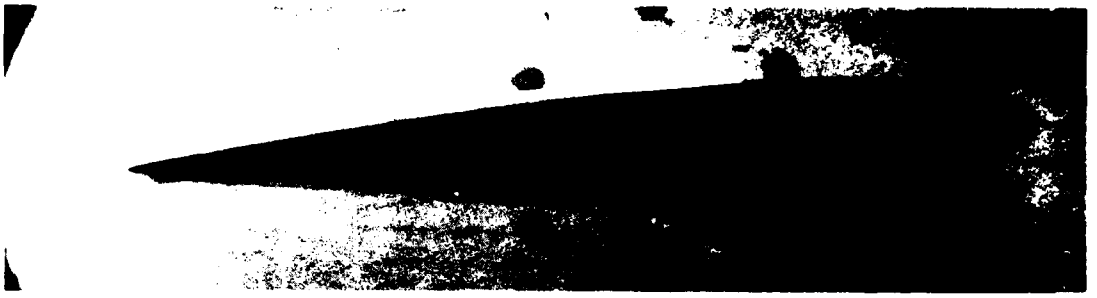

α = 4° (Neg. no. C99 16)

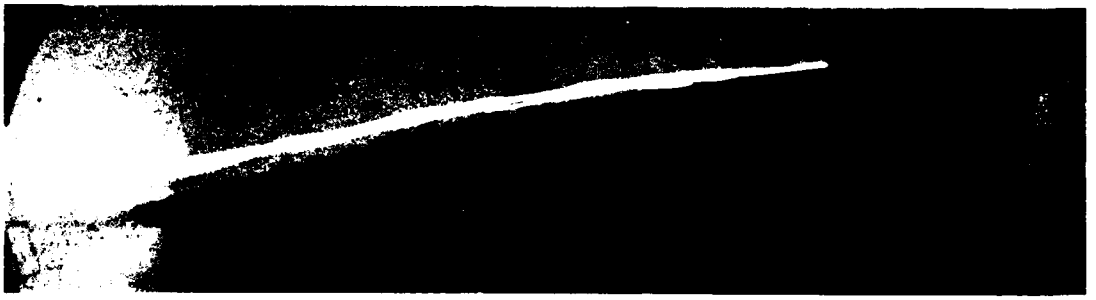

α = 8° (Neg. no. C99/7)

α = 12° (Neg no. C99/6)

α = 16° (Neg. no. C99/5)

FIG. 3(a) SQUARE TIP. VARIATION OF MAIN TIP VORTEX POSITION WITH INCIDENCE. SIDE VIEWS.

α = 4° (Neg. no. C98/12)

α = 8° (Neg. no. C98/11)

α = 12° (Neg. no. C98/10)

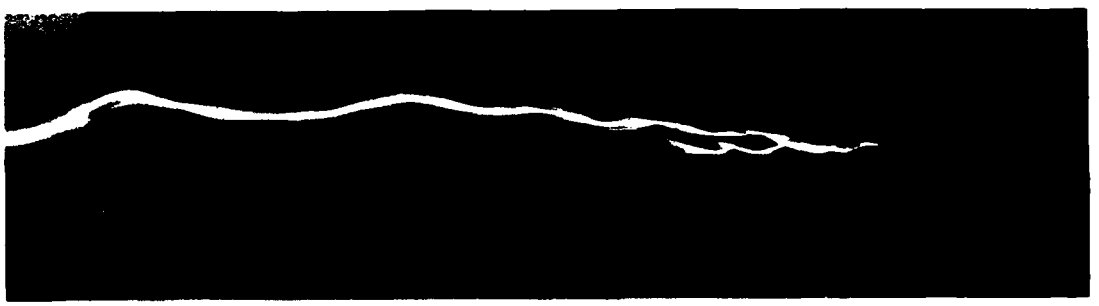

α = 16° (Neg. no. C98/9)

FIG. 3(b) SQUARE TIP. VARIATION OF MAIN TIP VORTEX POSITION WITH INCIDENCE. PLAN VIEWS.

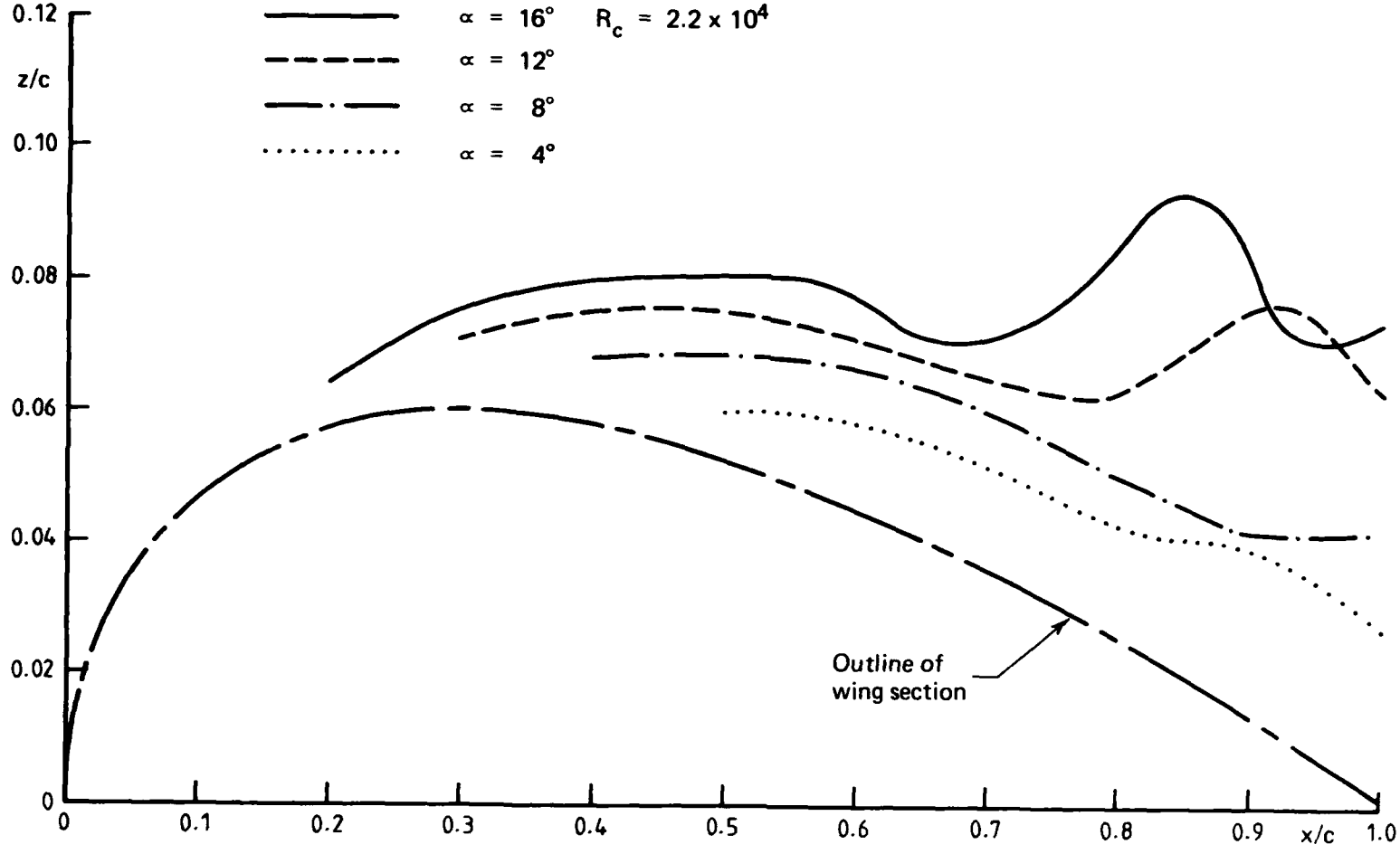

FIG. 4(a) SQUARE TIP. VARIATION OF MAIN TIP VORTEX POSITION WITH INCIDENCE. SIDE VIEW

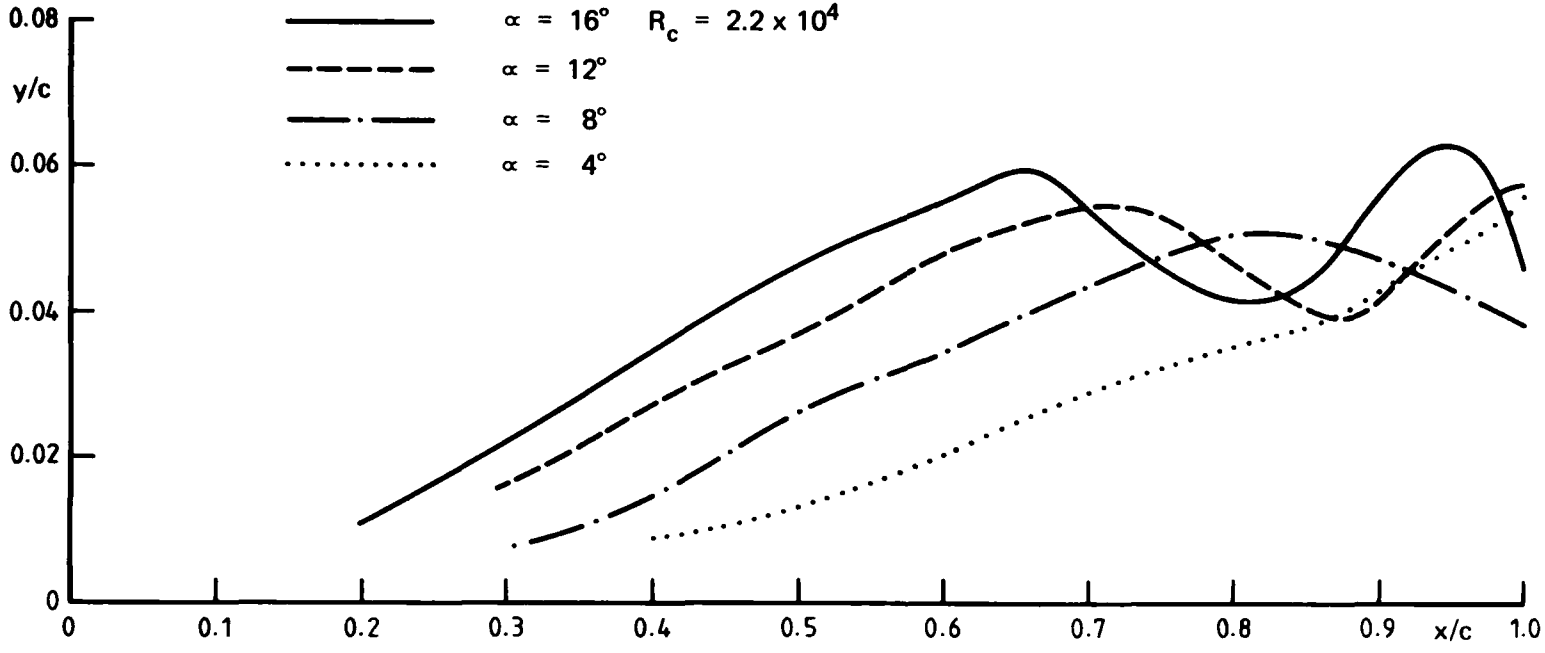

FIG. 4(b) SQUARE TIP. VARIATION OF MAIN TIP VORTEX POSITION WITH INCIDENCE. PLAN VIEW.

(Neg. no. C92/14)

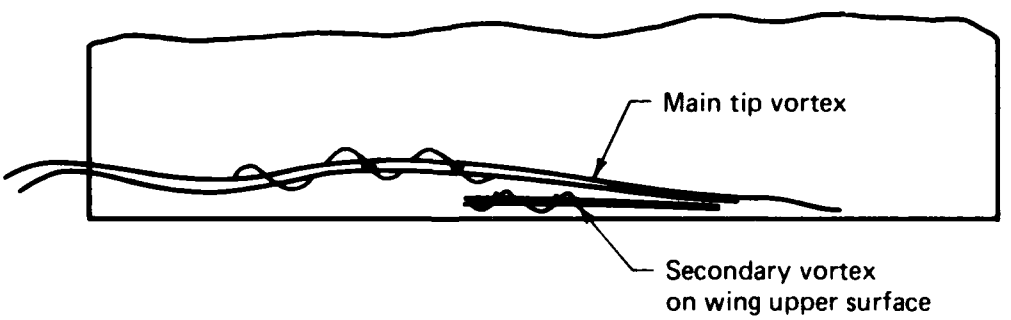

FIG. 5 SQUARE TIP. SECONDARY VORTEX ON WING UPPER SURFACE AT TIP. α = 16°.

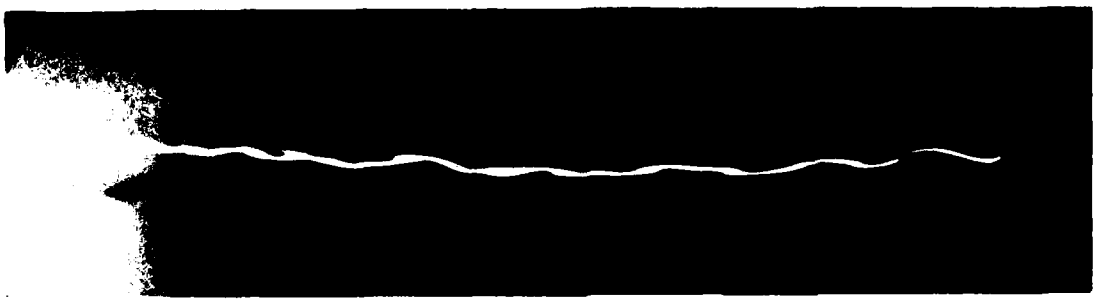

α = 4° (Neg. no. C96/5)

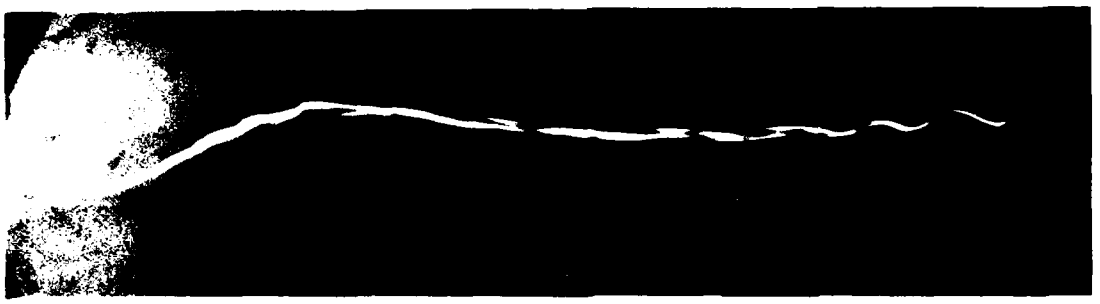

α = 8° (Neg. no. C96/4)

α = 12° (Neg. no. C96/3)

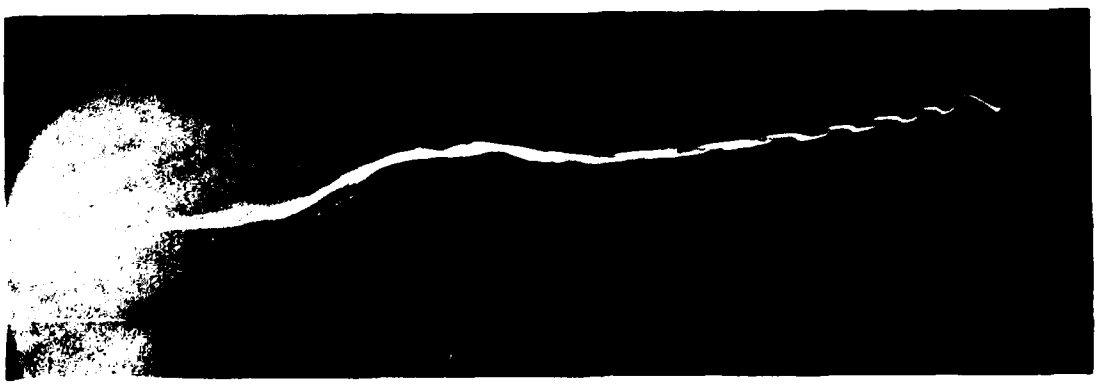

α = 16° (Neg. no. C96/12)

FIG. 6(a) SQUARE TIP. VARIATION OF FIRST TIP FACE VORTEX POSITION WITH INCIDENCE. SIDE VIEWS.

α = 4° (Neg. no. C97/4)

α = 8° (Neg. no. C97/3)

α = 12° (Neg. no. C97/2)

α = 16° (Neg. no. C97/1)

FIG. 6(b) SQUARE TIP. VARIATION OF FIRST TIP FACE VORTEX POSITION WITH INCIDENCE. PLAN VIEWS.

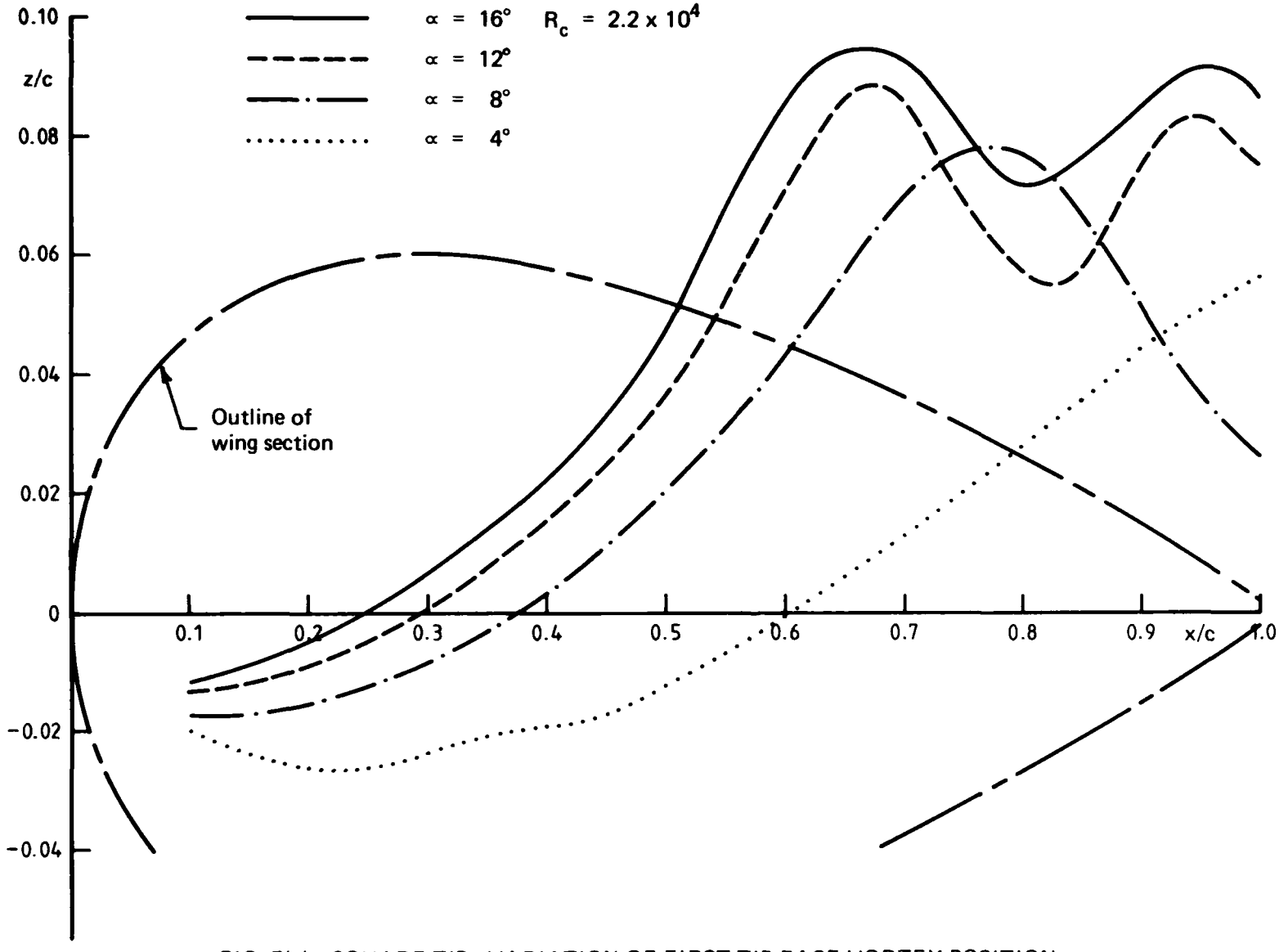

FIG. 7(a) SQUARE TIP. VARIATION OF FIRST TIP FACE VORTEX POSITION WITH INCIDENCE. SIDE VIEW.

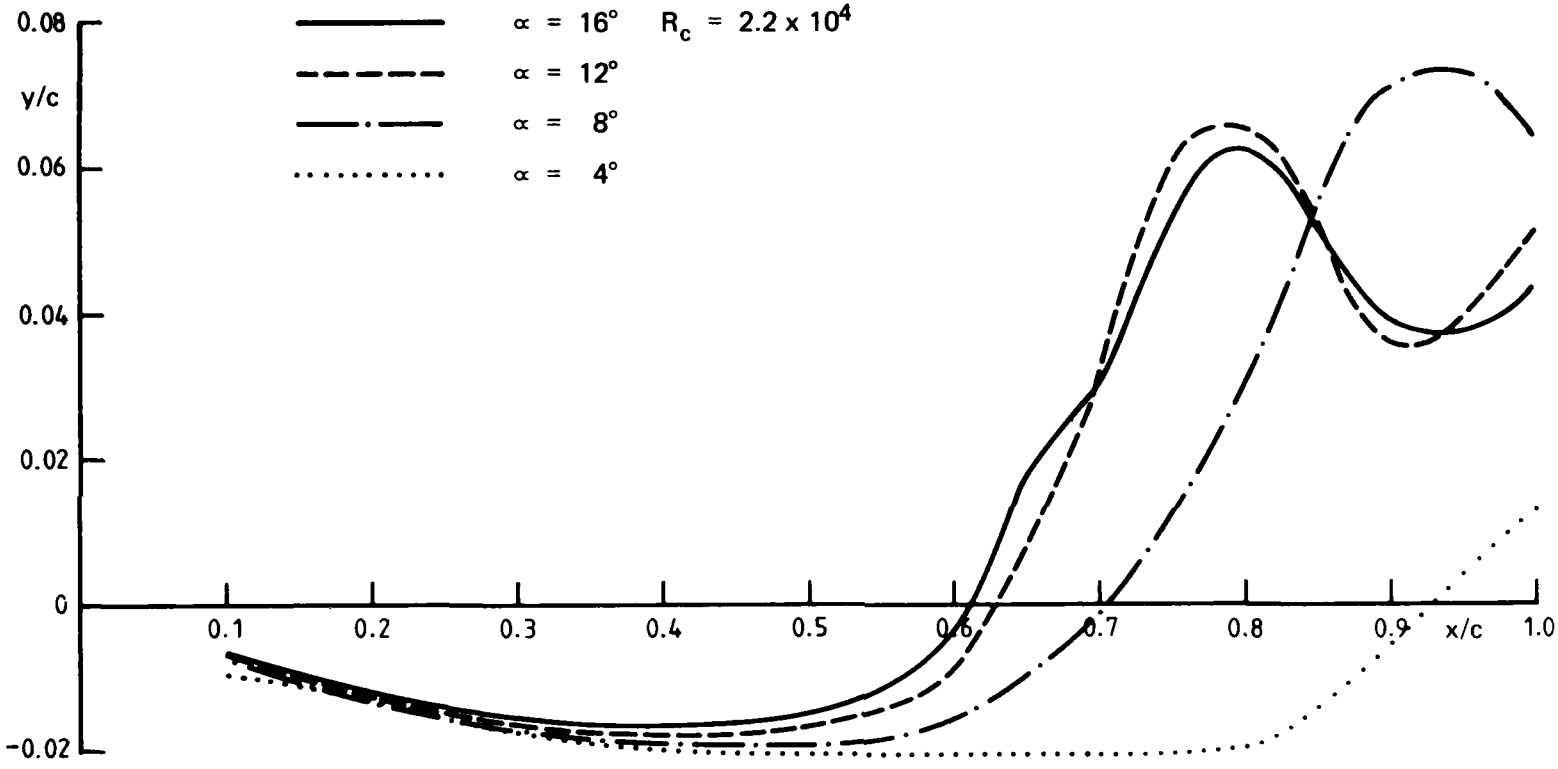

FIG. 7(b) SQUARE TIP. VARIATION OF FIRST TIP FACE VORTEX POSITION WITH INCIDENCE. PLAN VIEW.

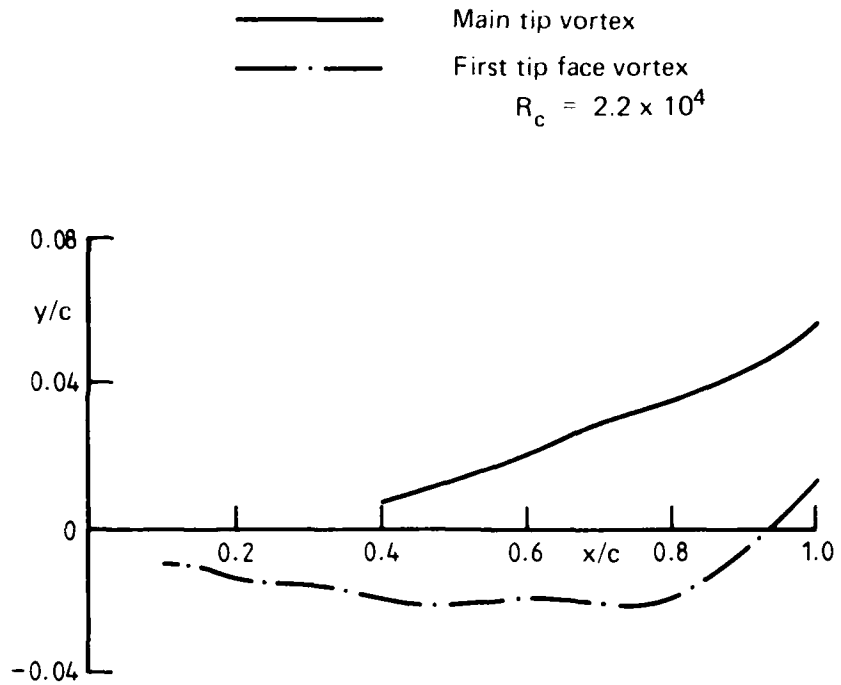

(a) $\alpha = 4°$

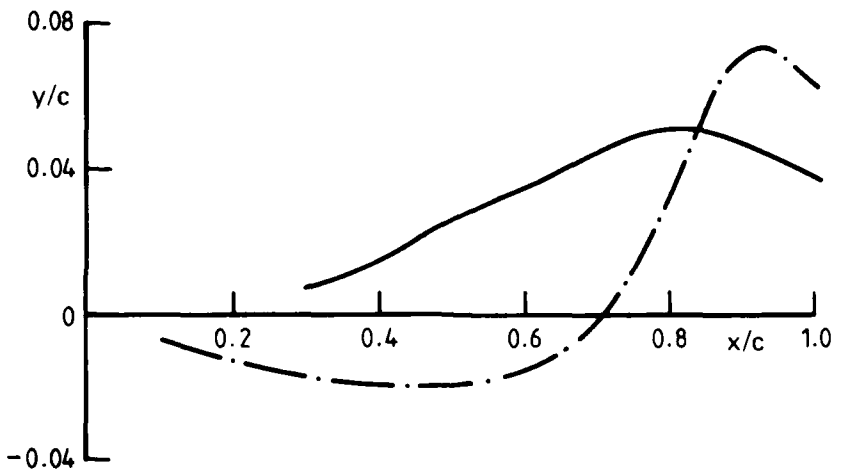

(b) $\alpha = 8°$

FIG. 8(a) & (b) SQUARE TIP. INTERACTION BETWEEN MAIN TIP VORTEX AND FIRST TIP FACE VORTEX. PLAN VIEW.

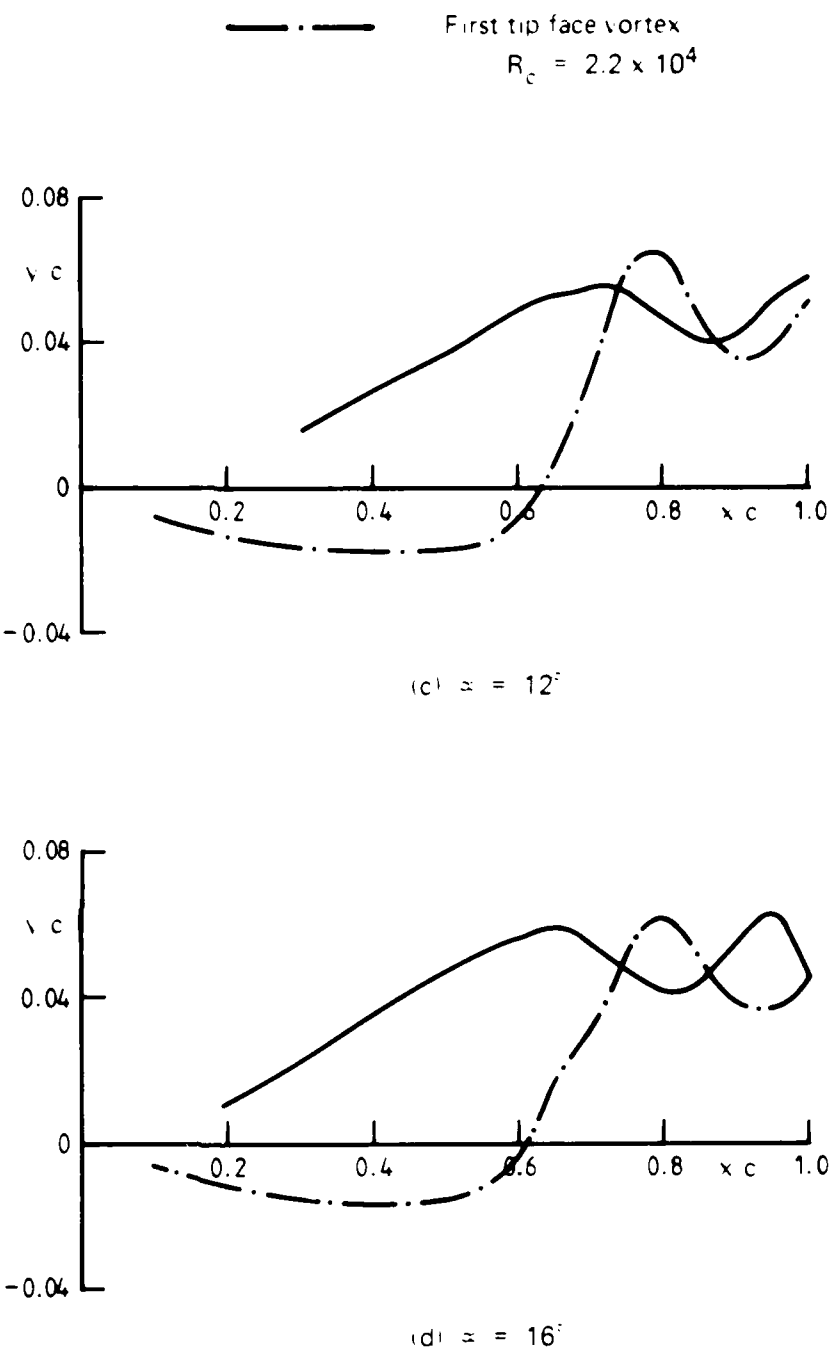

FIG. 8(c) & (d) SQUARE TIP. INTERACTION BETWEEN MAIN TIP VOR AND FIRST TIP FACE VORTEX. PLAN VIEW.

(Neg. no. C83/8)

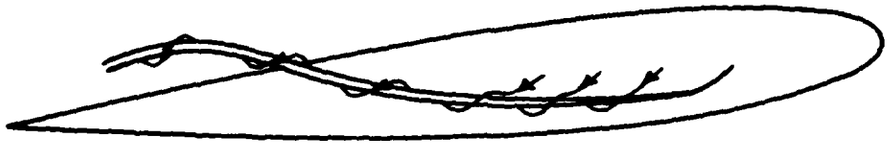

FIG. 9 SQUARE TIP. SECONDARY VORTEX ON TIP FACE. $\alpha = 8°$.

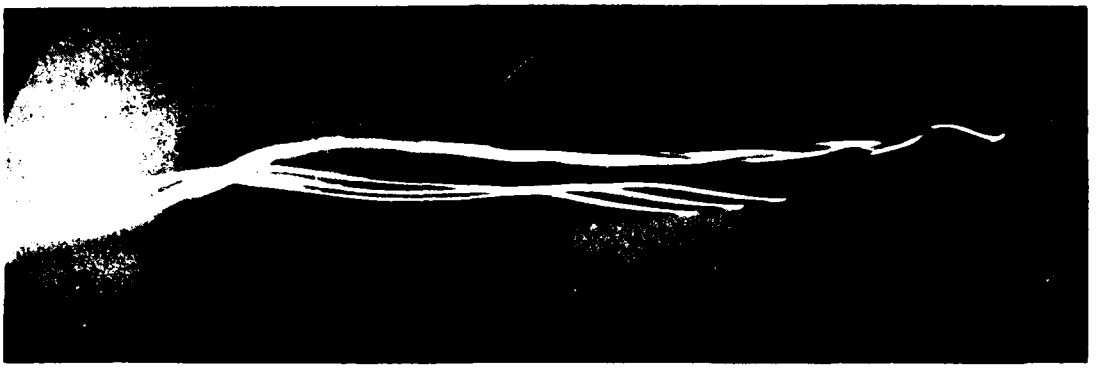

α = 8° (Neg. no. D1/3)

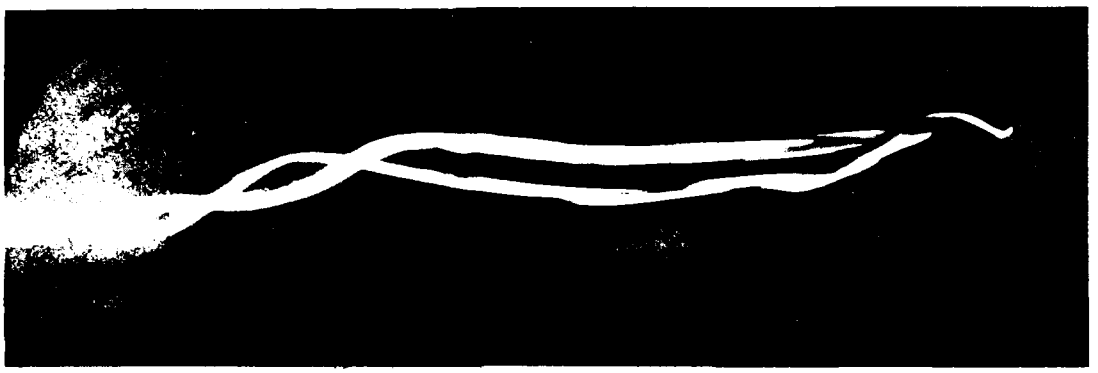

α = 12° (Neg. no. D1/2)

α = 16° (Neg. no. D1/1)

FIG. 10 SQUARE TIP. VARIATION OF SECOND TIP FACE VORTEX POSITION WITH INCIDENCE. SIDE VIEWS.

(Neg. no. B92/2)

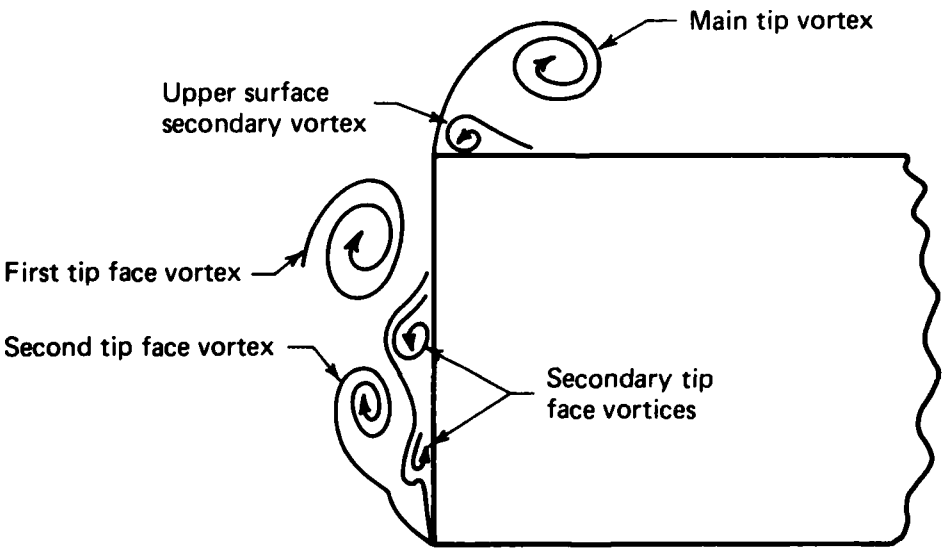

FIG. 11(a) SQUARE TIP. CROSSFLOW SECTION THROUGH TIP VORTEX SYSTEM. α = 12°, x/c = 0.5. DYE TECHNIQUE.

x/c = 0.1 (Neg. no. D7/2)

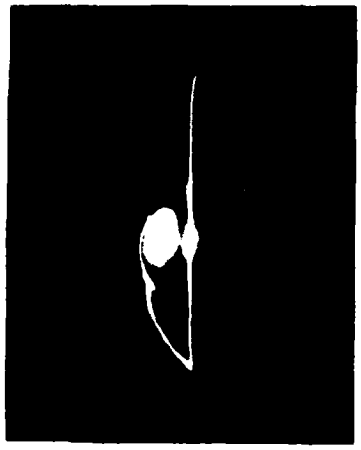

x/c = 0.2 (Neg. no. D7/4)

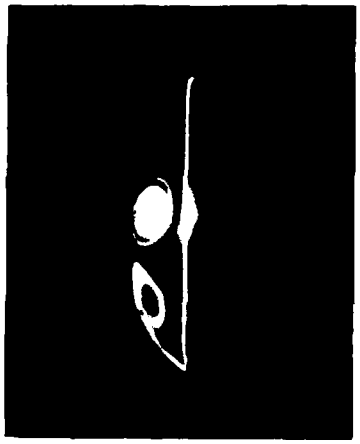

x/c = 0.3 (Neg. no. D7/16)

x/c = 0.4 (Neg. no. D7/15)

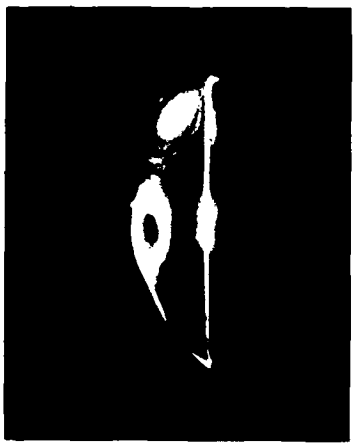

x/c = 0.5 (Neg. no. D7/14)

x/c = 0.6 (Neg. no. D7/13)

FIG. 11(b) SQUARE TIP. CROSSFLOW SECTIONS THROUGH TIP FACE VORTICES. α = 16°. HYDROGEN BUBBLE TECHNIQUE.

α = 8° (Neg. no. C90/14)

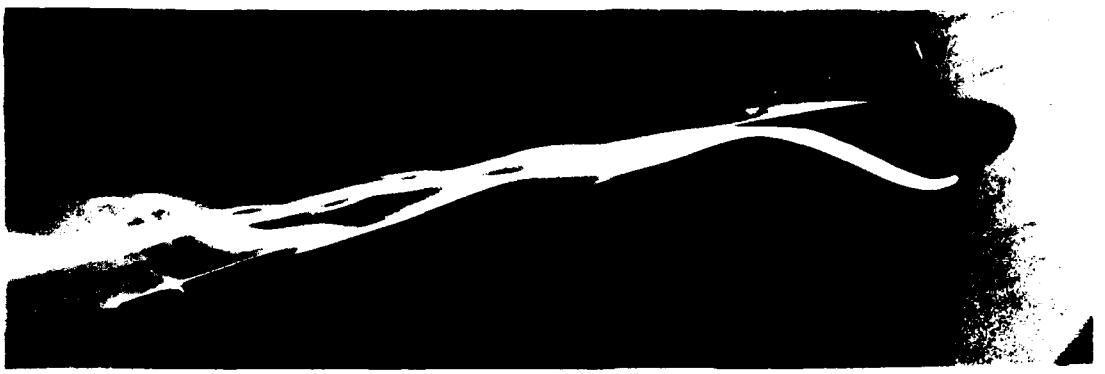

α = 12° (Neg. no. C90/12)

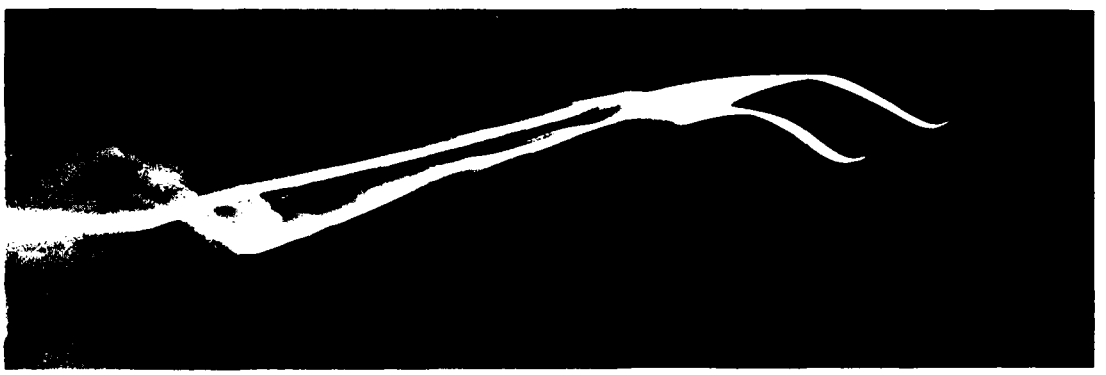

α = 16° (Neg. no. C90/10)

FIG. 12(a) ROUNDED TIP. VARIATION OF MAIN TIP VORTEX POSITION WITH INCIDENCE. SIDE VIEWS.

α = 8° (Neg. no. C91/3)

α = 12° (Neg. no. C91/1)

α = 16° (Neg. no. C91/15)

FIG. 12(b) ROUNDED TIP. VARIATION OF MAIN TIP VORTEX POSITION WITH INCIDENCE. PLAN VIEWS.

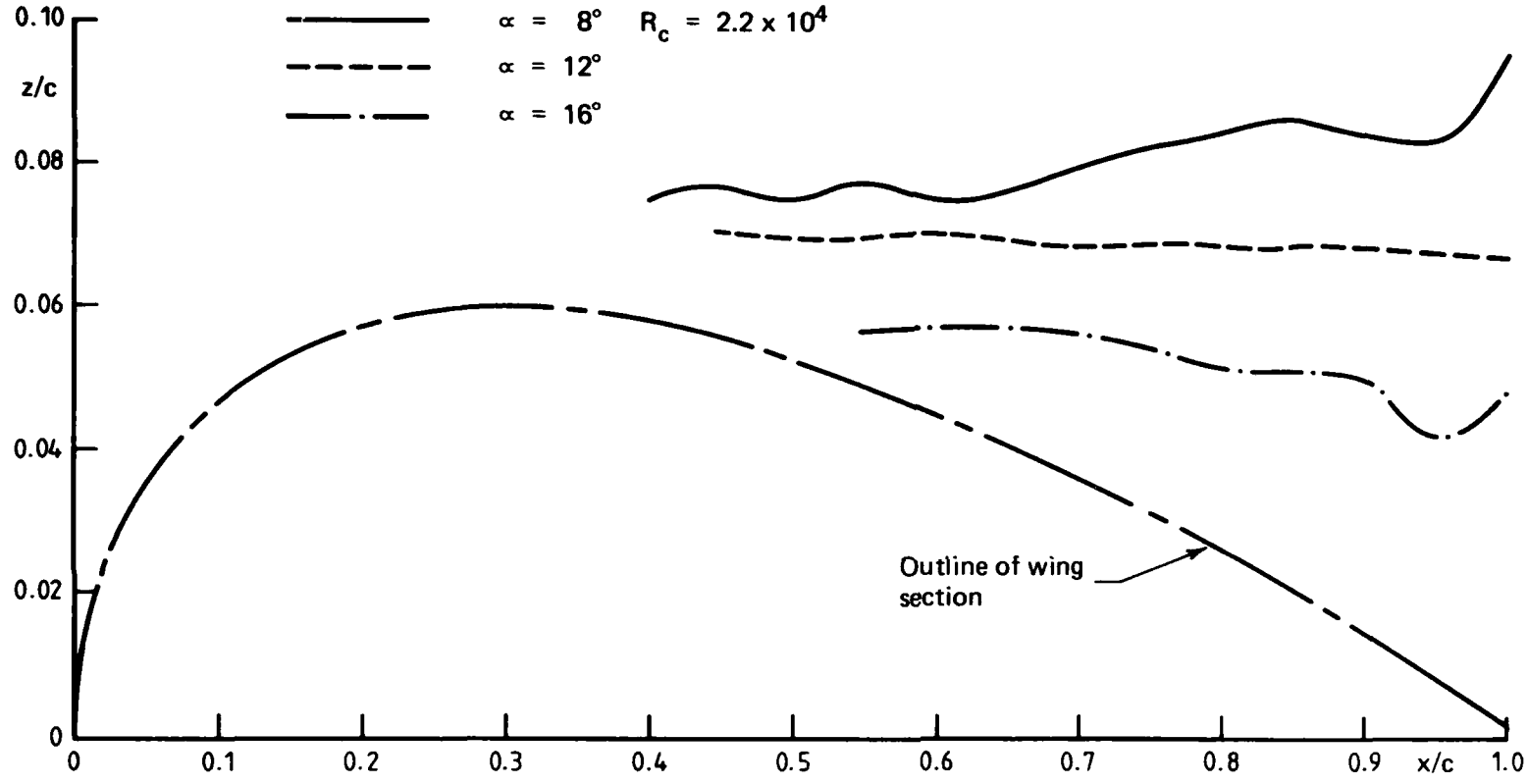

FIG. 13(a) ROUNDED TIP. VARIATION OF MAIN TIP VORTEX POSITION WITH INCIDENCE. SIDE VIEW.

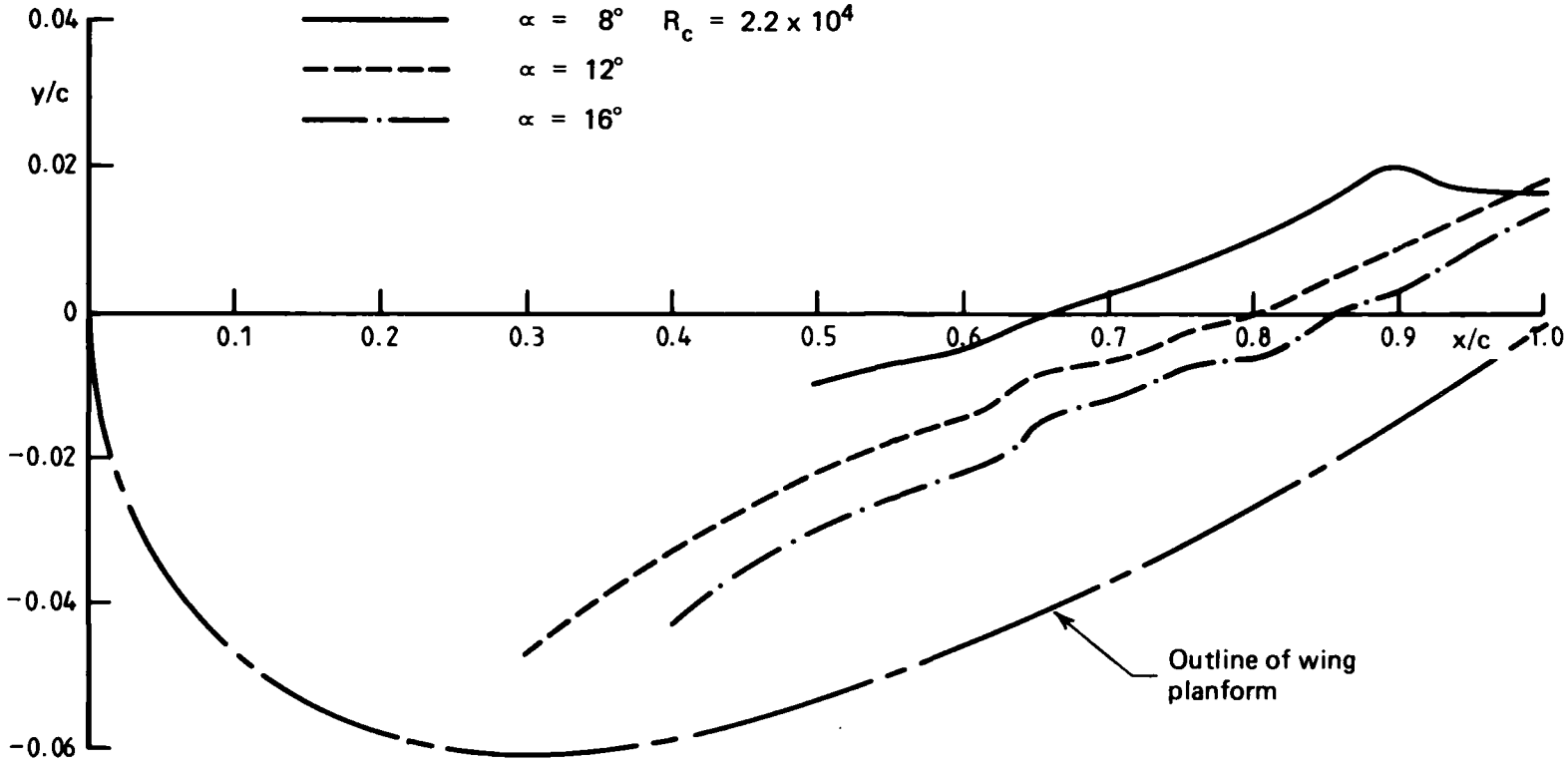

FIG. 13(b) ROUNDED TIP. VARIATION OF MAIN TIP VORTEX POSITION WITH INCIDENCE. PLAN VIEW.

(Neg. no. B95/1)

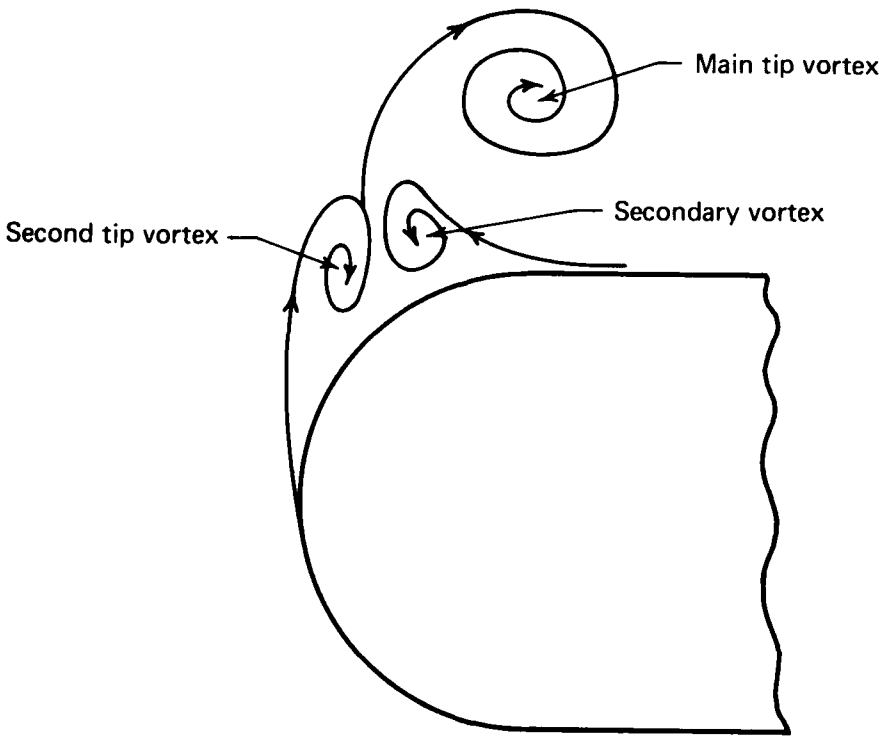

FIG. 14 ROUNDED TIP. CROSSFLOW SECTION THROUGH TIP VORTEX SYSTEM. α = 16°, x/c = 0.6. DYE TECHNIQUE.

α = 4° (Neg. no. B100/5)

α = 8° (Neg. no. B100/6)

α = 12° (Neg. no. B100/7)

α = 16° (Neg. no. B100/8)

FIG. 15(a) BEVELLED TIP. VARIATION OF MAIN TIP VORTEX POSITION WITH INCIDENCE. SIDE VIEWS.

α = 4° (Neg. no. C1/5)

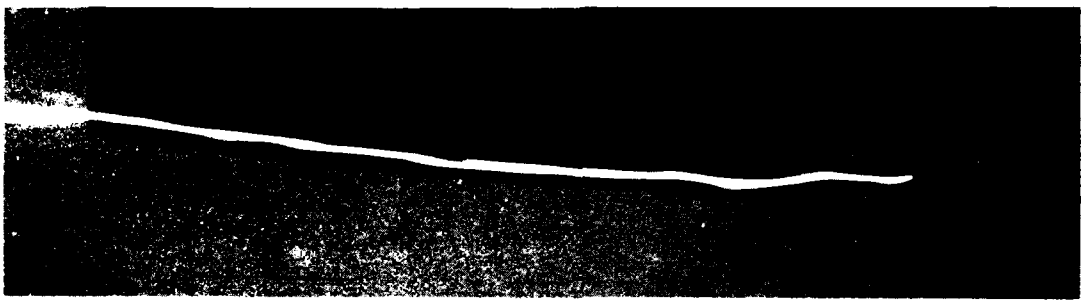

α = 8° (Neg. no. C1/6)

α = 12° (Neg. no. C1/7)

α = 16° (Neg. no. C1/8)

FIG. 15(b) BEVELLED TIP. VARIATION OF MAIN TIP VORTEX POSITION WITH INCIDENCE. PLAN VIEWS.

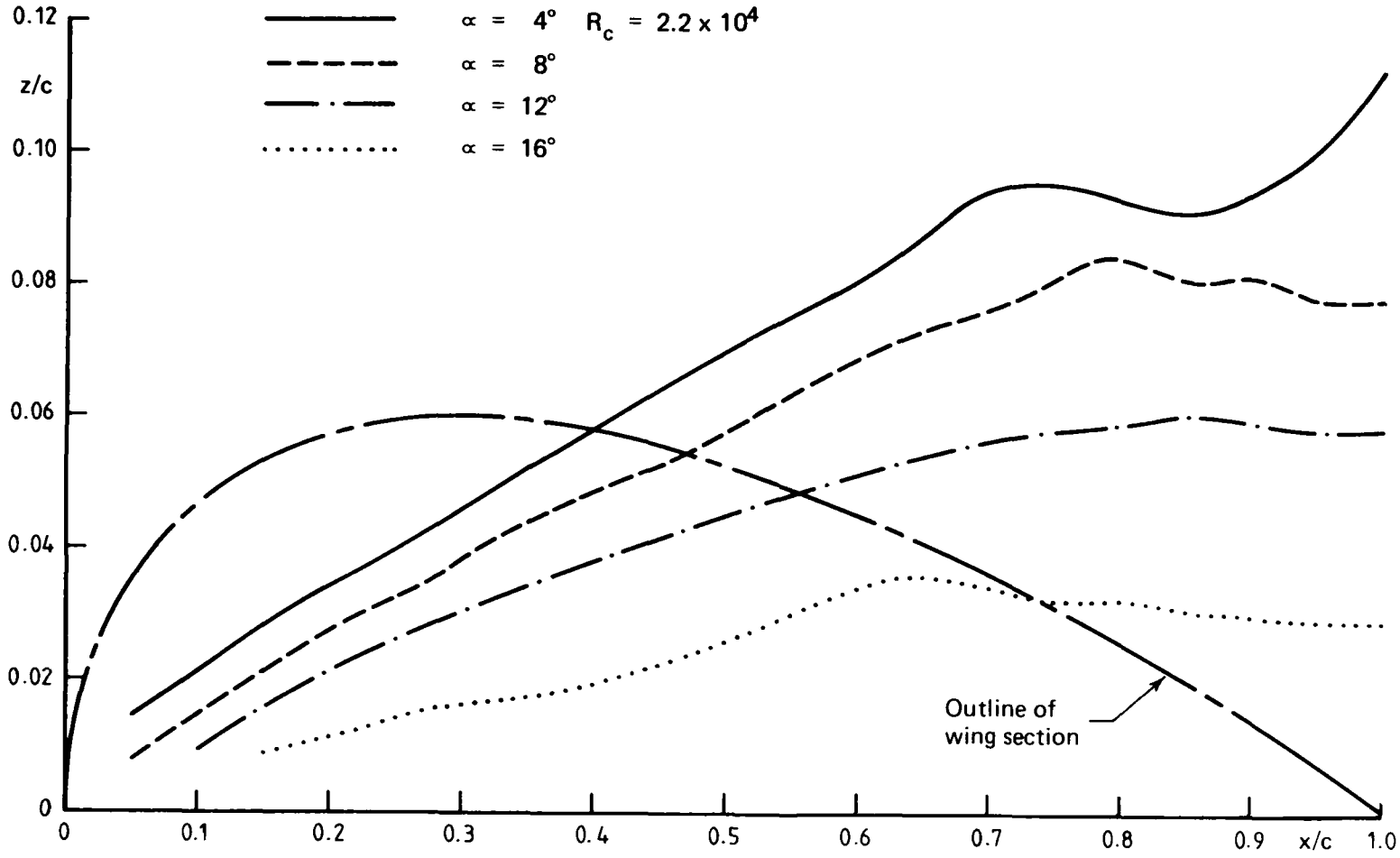

FIG. 16(a) BEVELLED TIP. VARIATION OF MAIN TIP VORTEX POSITION WITH INCIDENCE. SIDE VIEW.

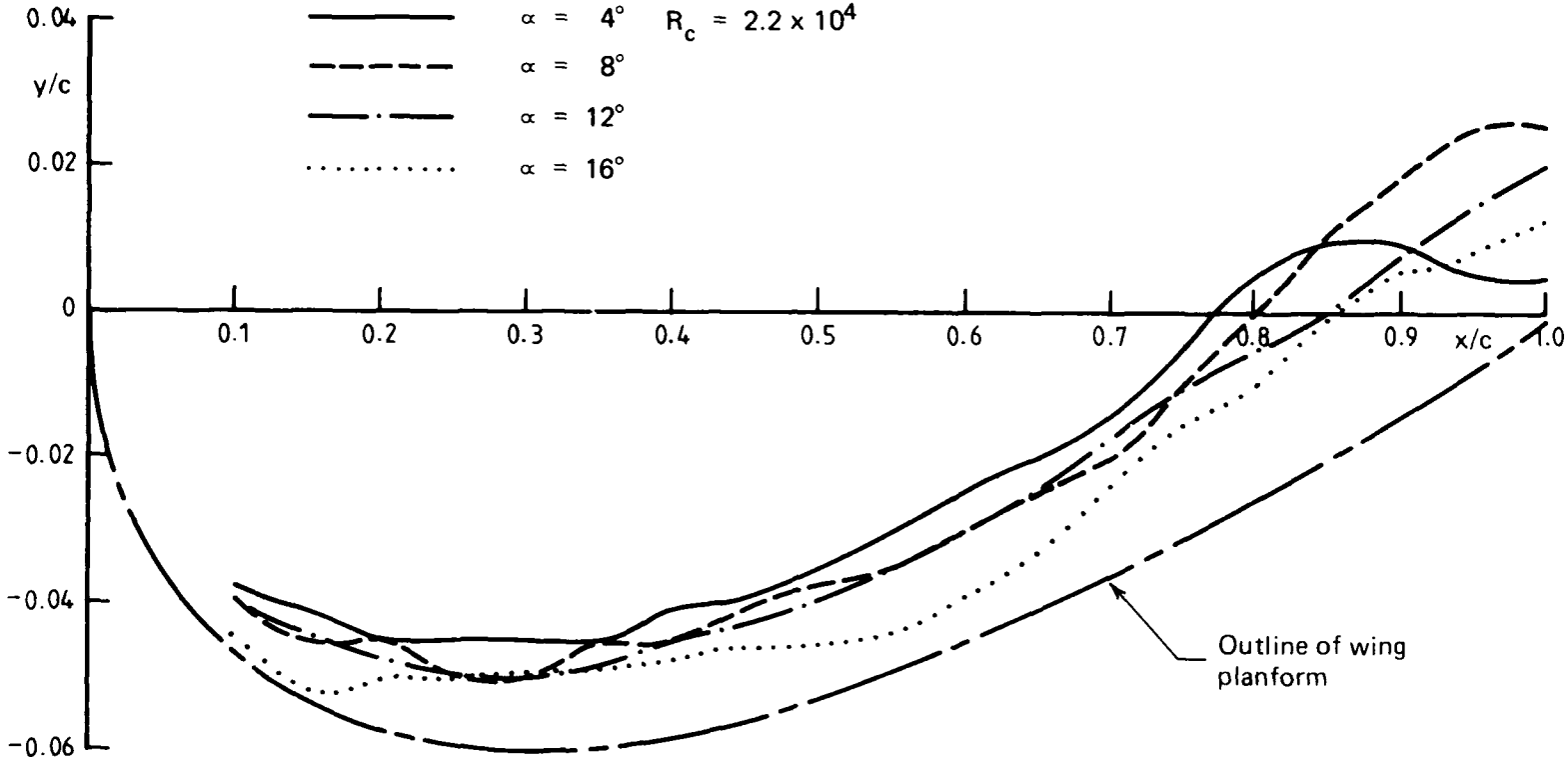

FIG. 16(b) BEVELLED TIP. VARIATION OF MAIN TIP VORTEX POSITION WITH INCIDENCE. PLAN VIEW

(Neg. no. B97/3)

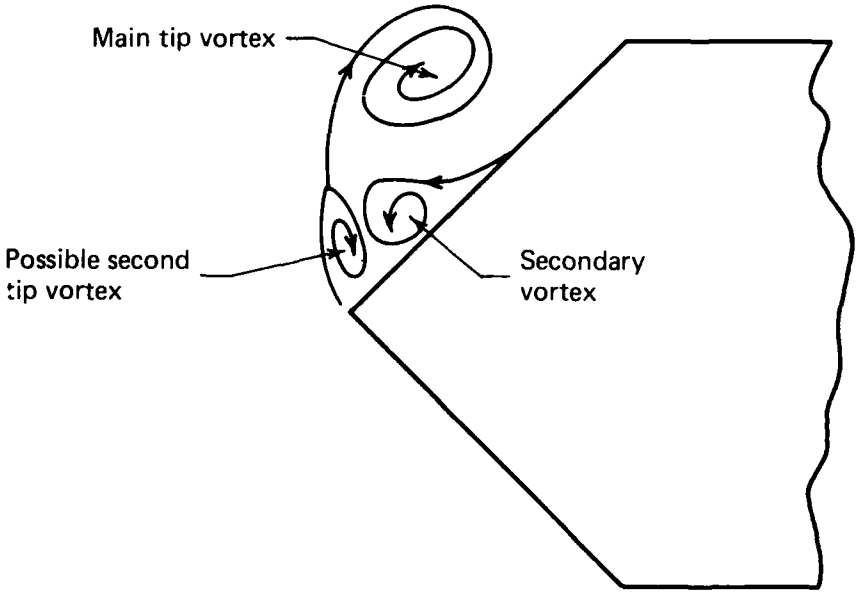

FIG. 17 BEVELLED TIP. CROSSFLOW SECTION THROUGH TIP VORT SYSTEM. α = 16°. x/c = 0.4. DYE TECHNIQUE.

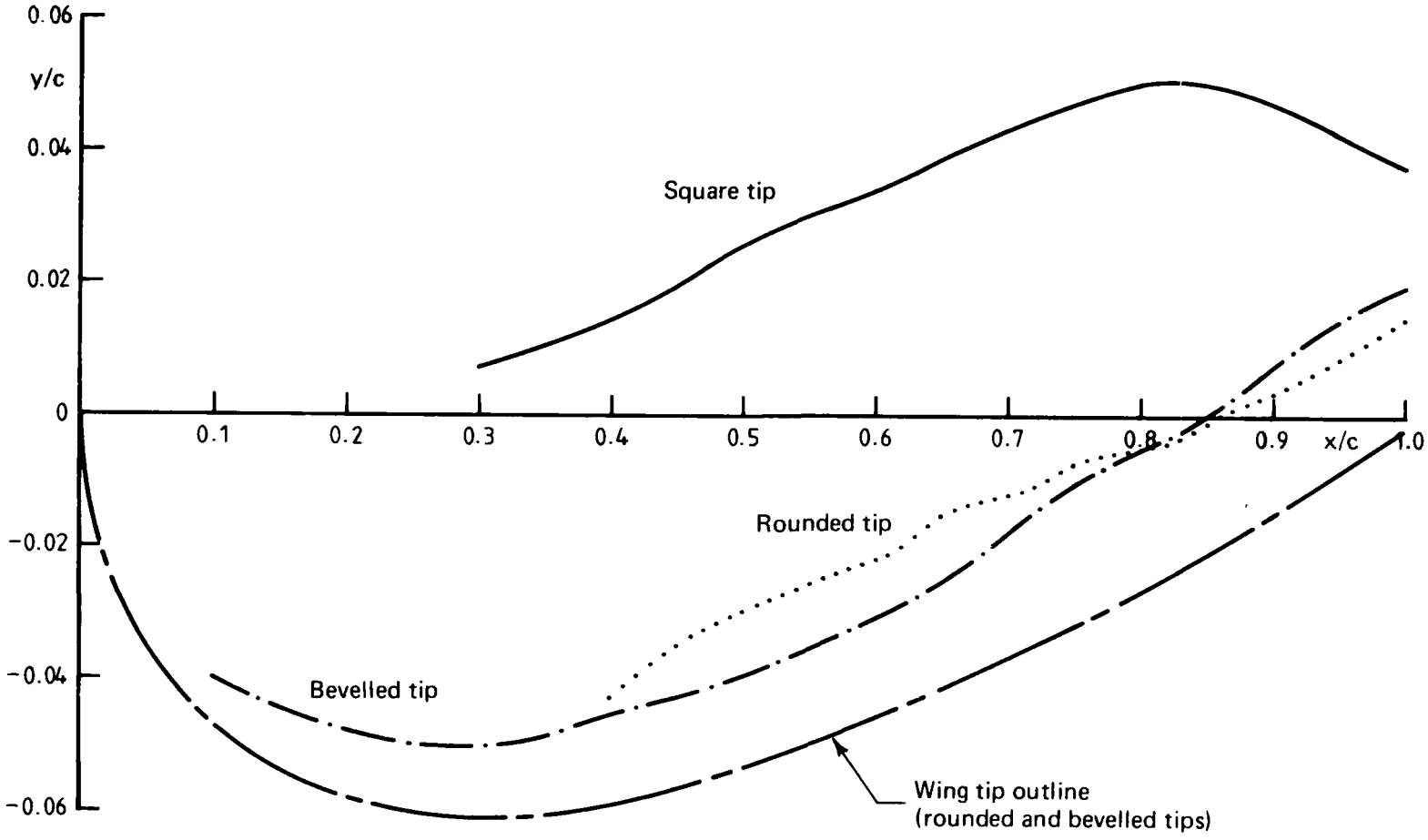

FIG. 18(a) COMPARISON OF MAIN TIP VORTEX POSITION FOR DIFFERENT TIP EDGE SHAPES. PLAN VIEW. INCIDENCE = 8°.

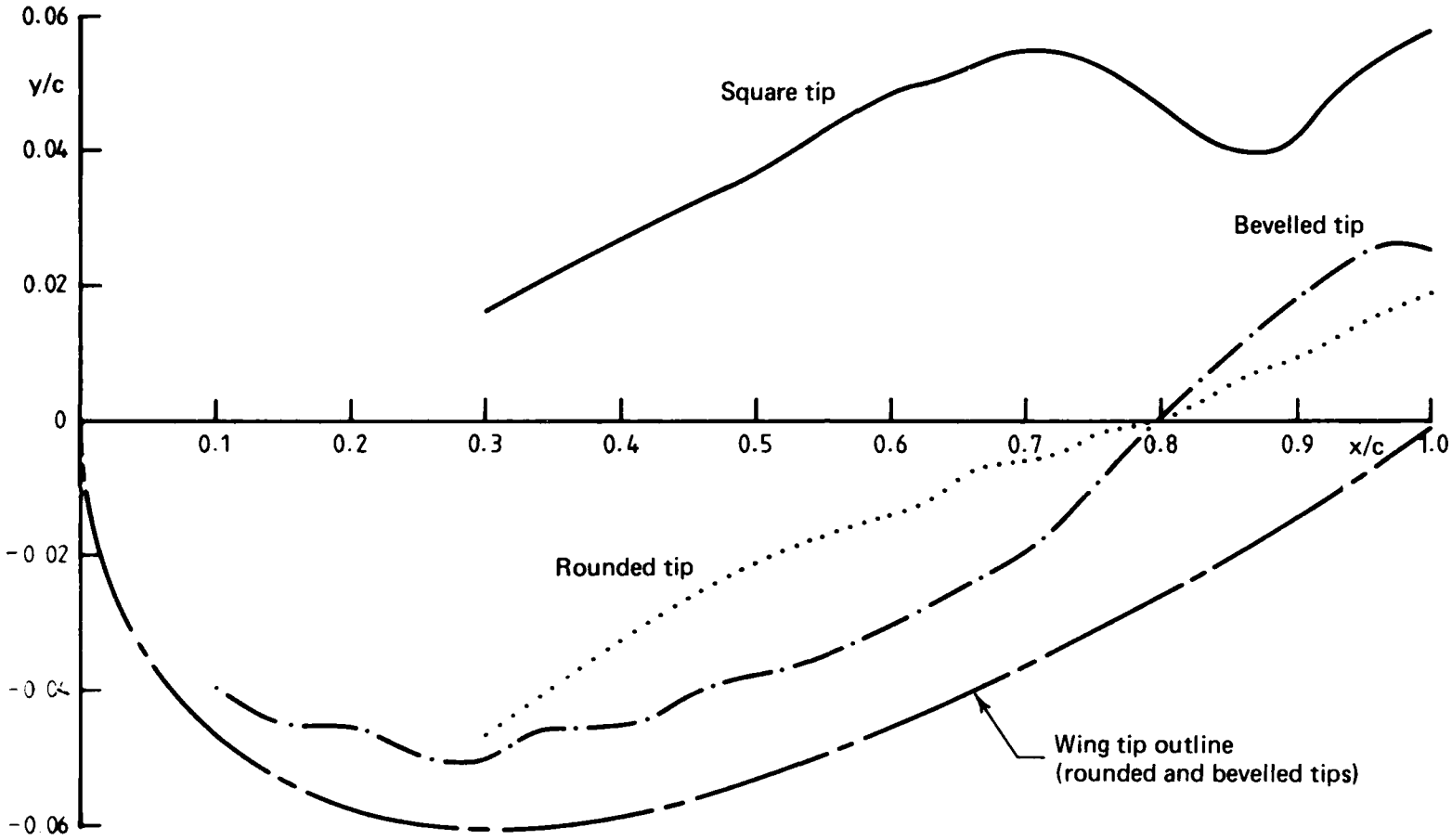

FIG. 18(b) COMPARISON OF MAIN TIP VORTEX POSITION FOR DIFFERENT TIP EDGE SHAPES. PLAN VIEW. INCIDENCE = 12°.

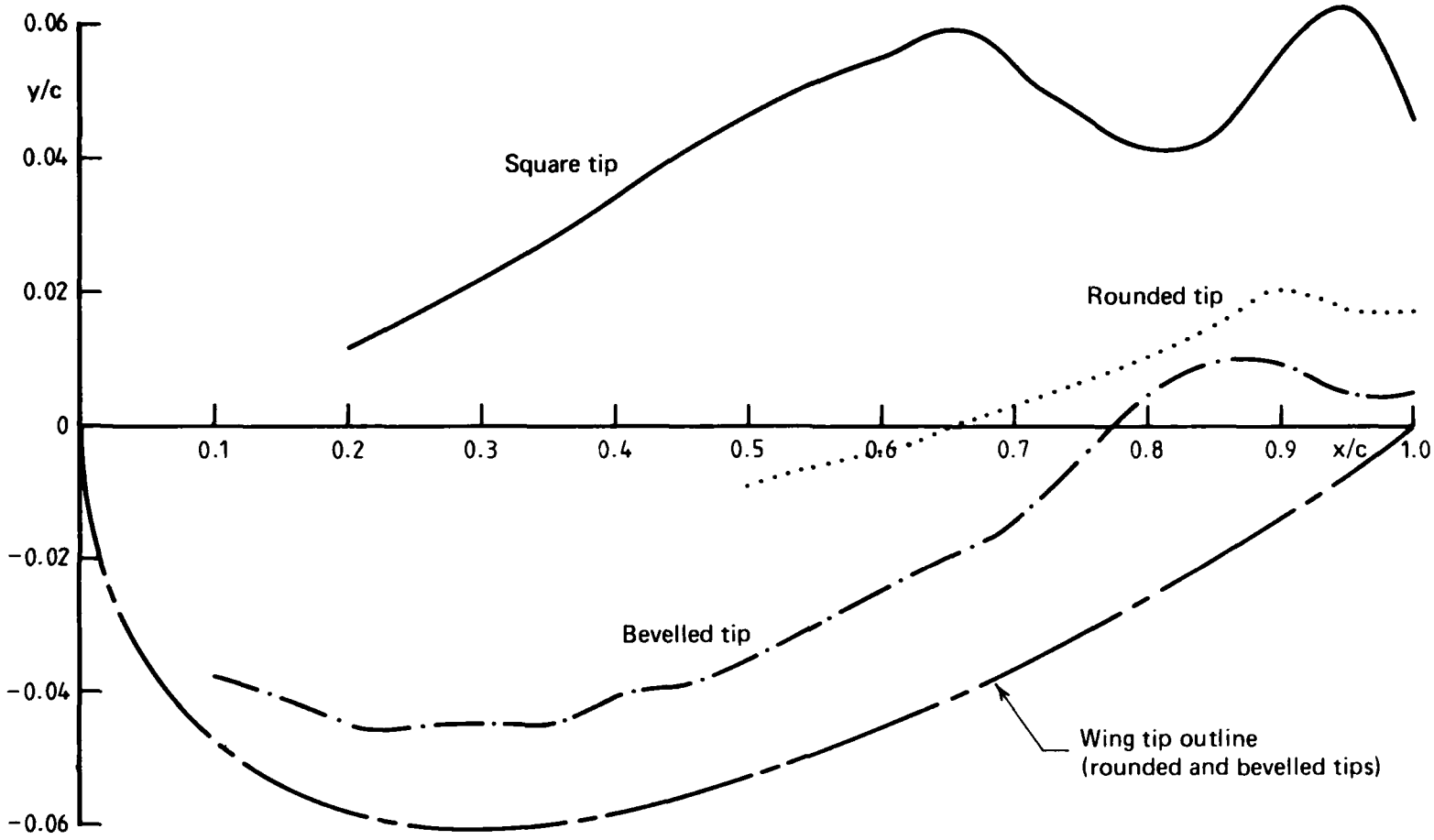

FIG. 18(c) COMPARISON OF MAIN TIP VORTEX POSITION FOR DIFFERENT TIP EDGE SHAPES. PLAN VIEW. INCIDENCE = 16°.

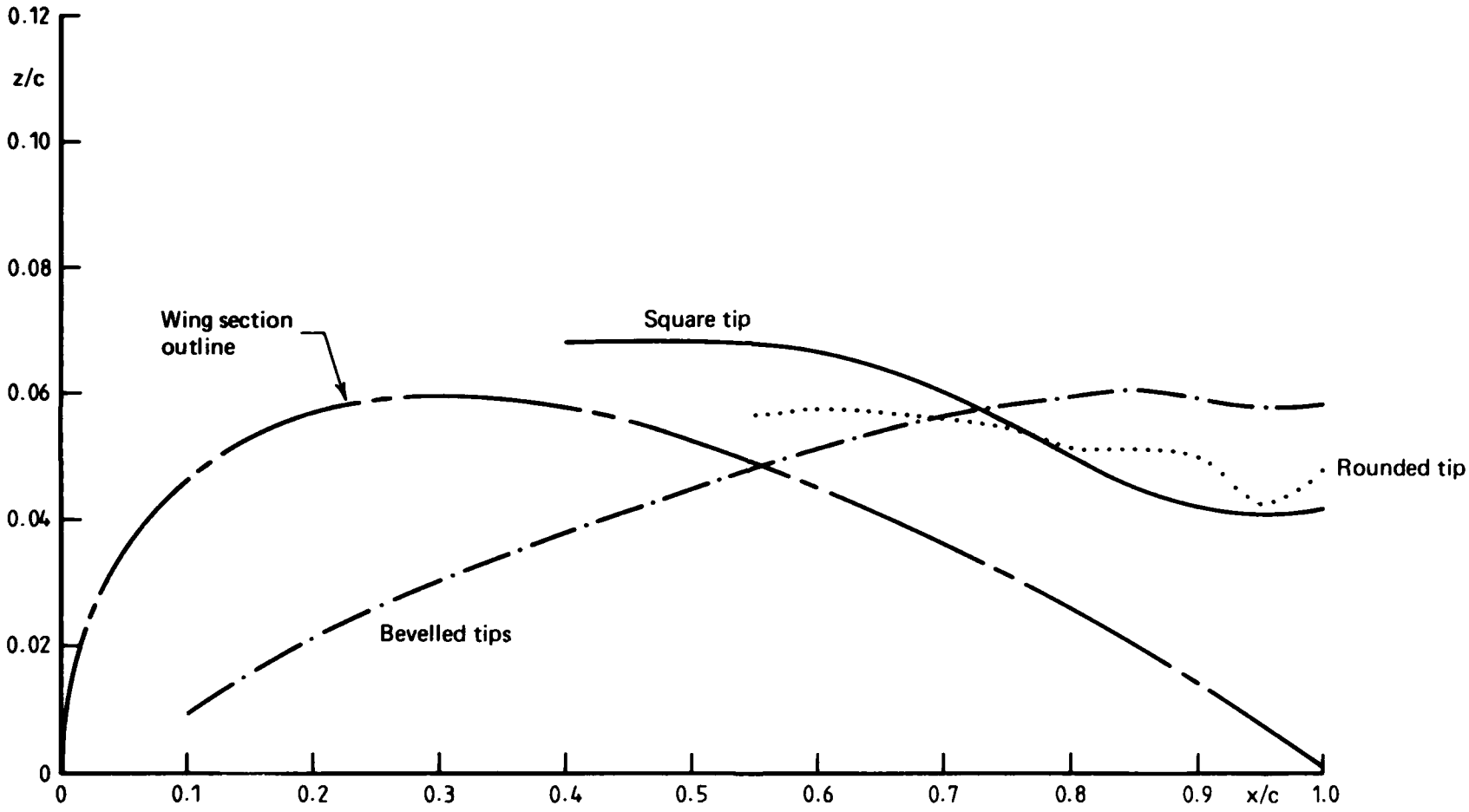

FIG. 19(a) COMPARISON OF MAIN TIP VORTEX POSITIONS FOR DIFFERENT TIP EDGE SHAPES. SIDE VIEW. INCIDENCE = 8°.

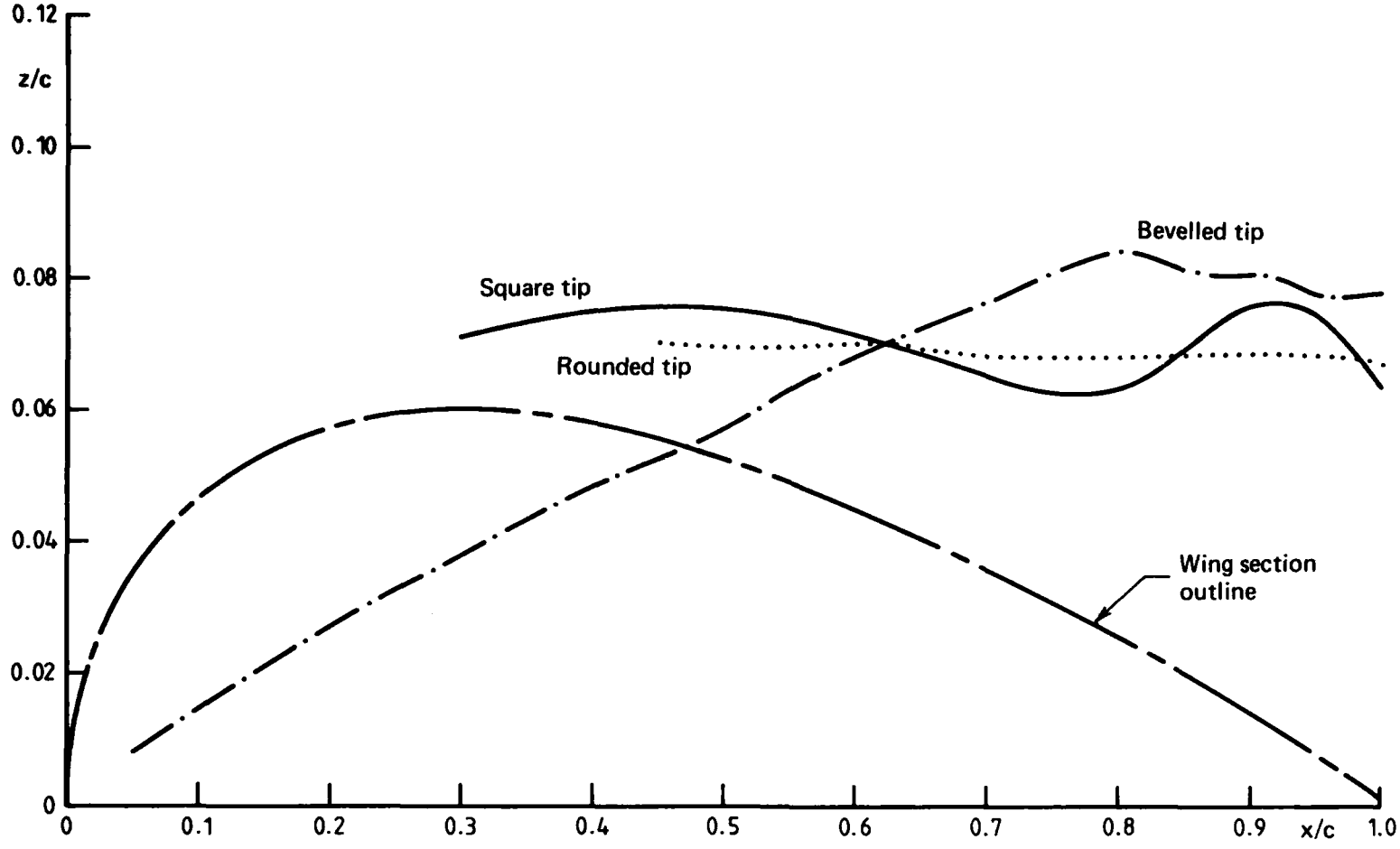

FIG. 19(b) COMPARISON OF MAIN TIP VORTEX POSITIONS FOR DIFFERENT TIP EDGE SHAPES. SIDE VIEW. INCIDENCE = 12°.

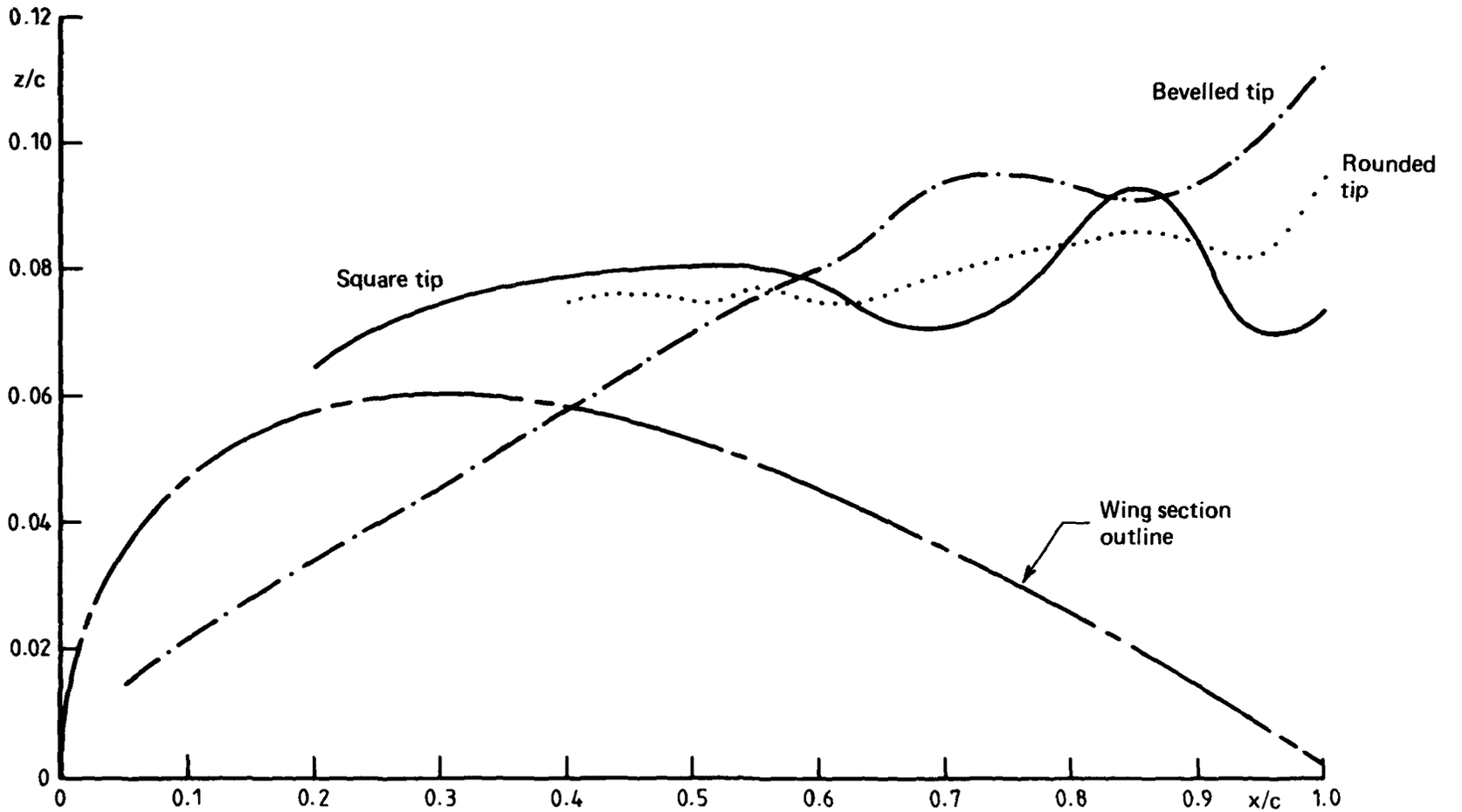

FIG. 19(c) COMPARISON OF MAIN TIP VORTEX POSITIONS FOR DIFFERENT TIP EDGE SHAPES. SIDE VIEW. INCIDENCE = 16°.

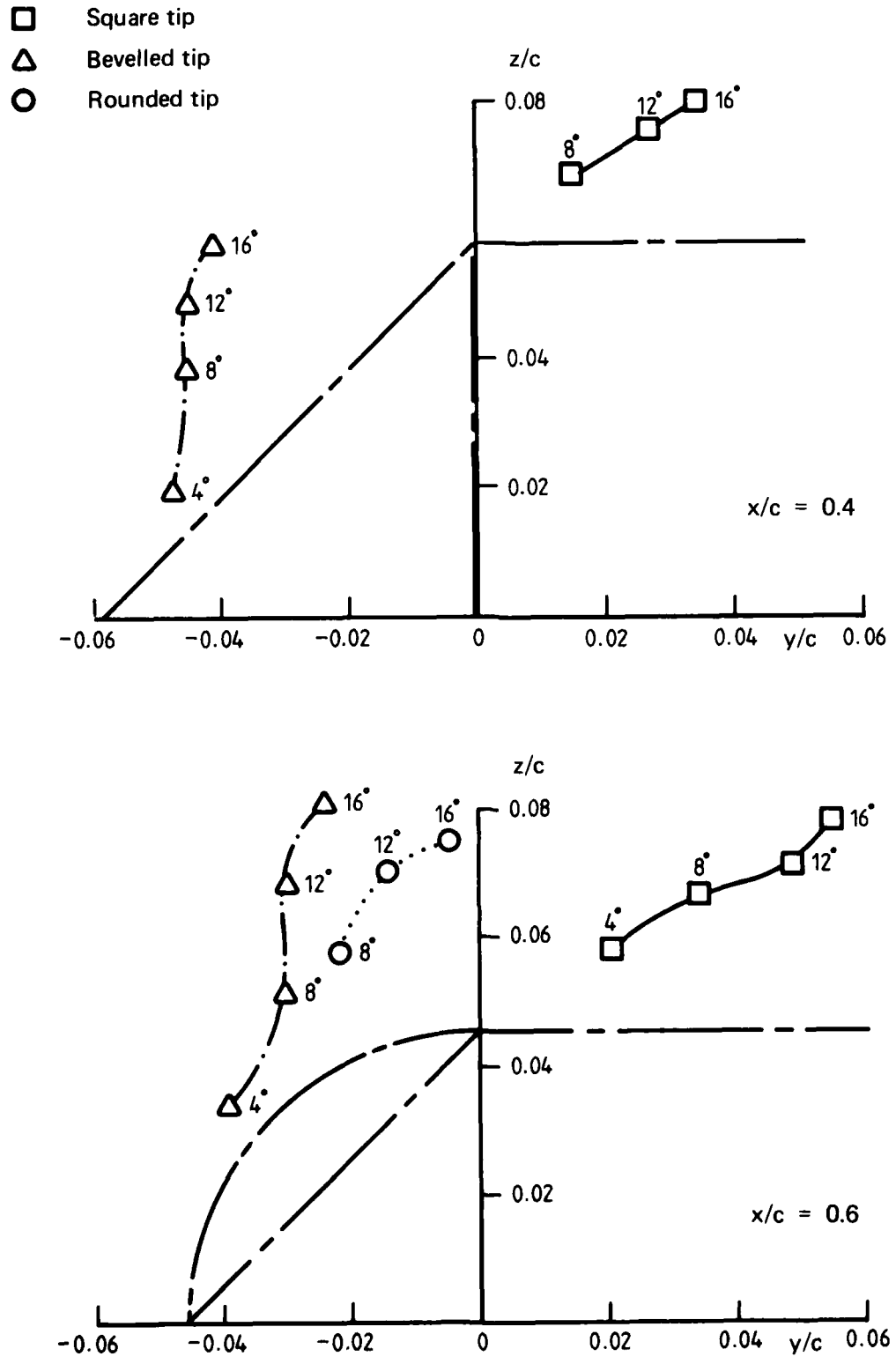

FIG. 20 COMPARISON OF MAIN TIP VORTEX POSITIONS FOR DIFFERENT TIP EDGE SHAPES.

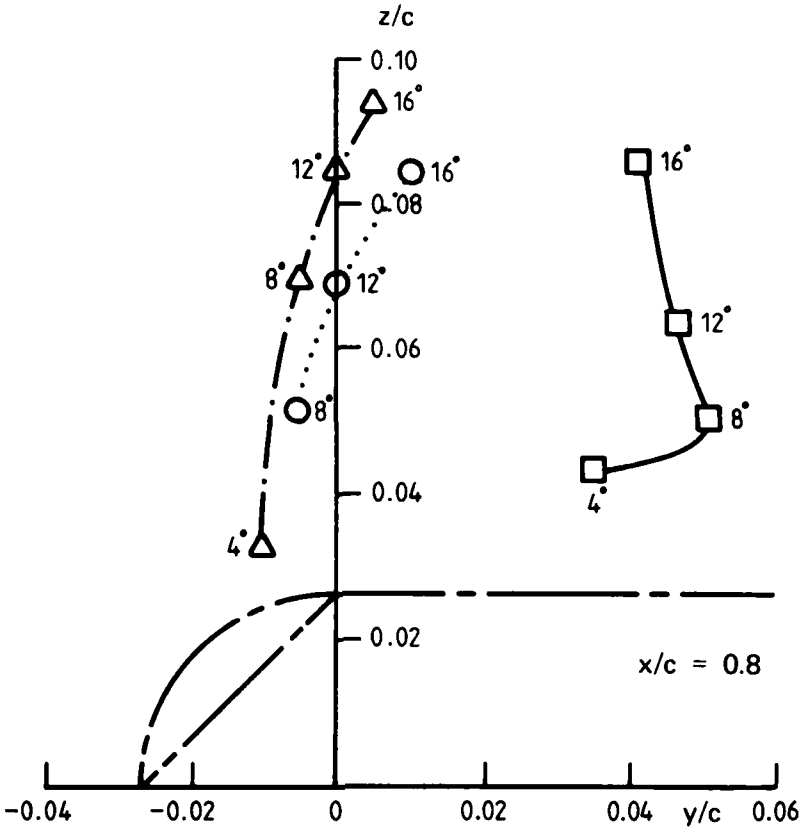
z/c
0.10
0.08
0.06
0.04
0.02
16°
12°
16°
8°
12°
8°
4°
16°
12°
8°
4°
x/c = 0.8
-0.04
-0.02
0
0.02
0.04
y/c
0.06

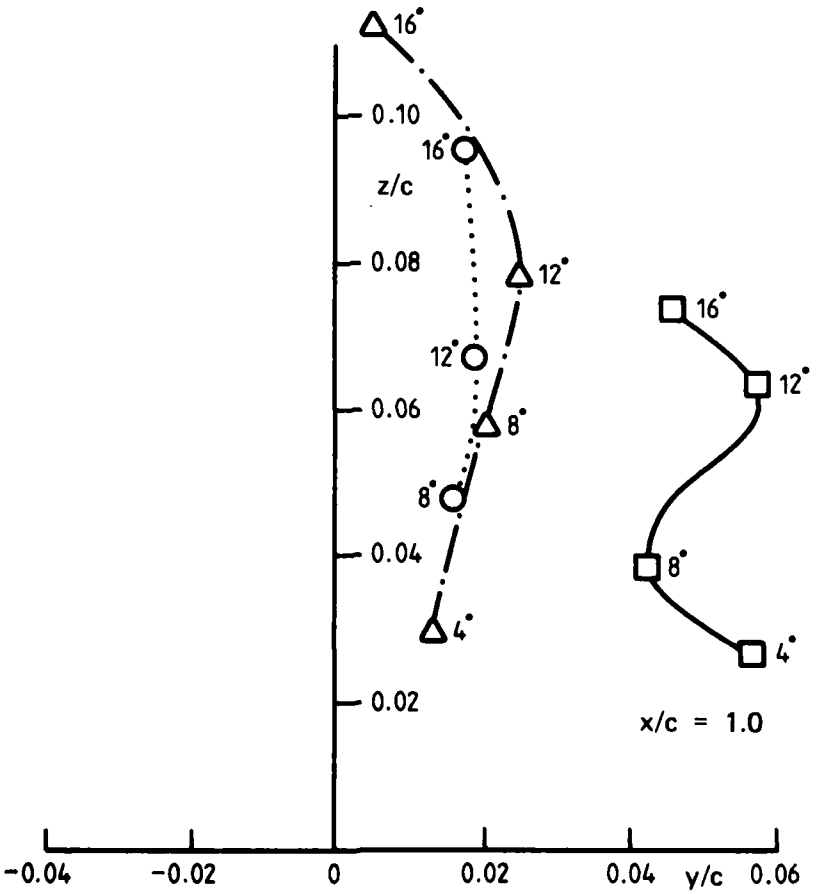
16°
0.10
16°
z/c
0.08
12°
12°
16°
0.06
8°
12°
8°
8°
0.04
4°
4°
0.02
x/c = 1.0
-0.04
-0.02
0
0.02
0.04
y/c
0.06

FIG. 20 (Contd.)

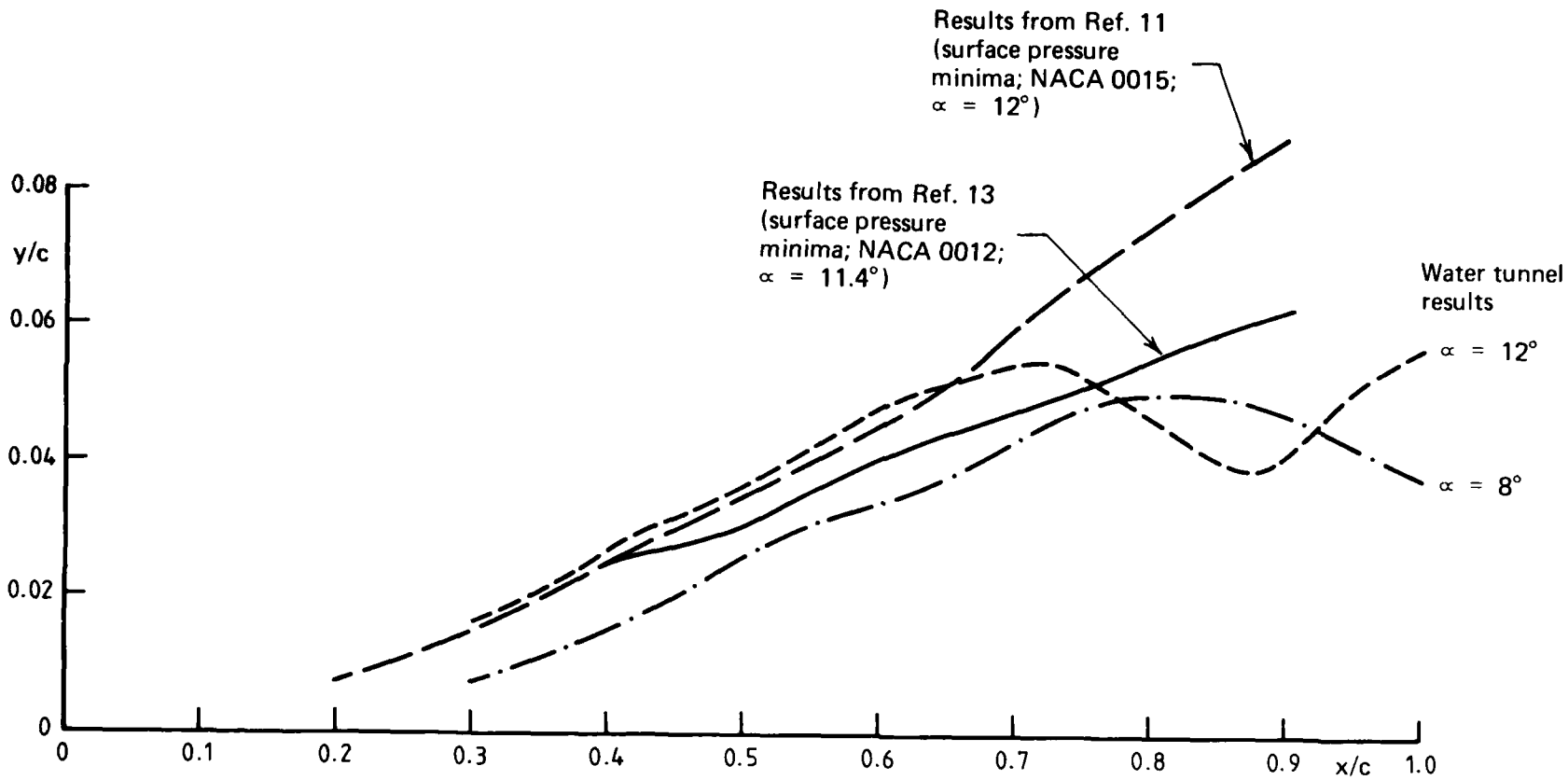

FIG. 21 COMPARISON OF MAIN TIP VORTEX TRAJECTORIES WITH WIND TUNNEL RESULTS. SQUARE TIP.

DISTRIBUTION

AUSTRALIA

DEPARTMENT OF DEFENCE

Central Office

Chief Defence Scientist
Deputy Chief Defence Scientist
Superintendent, Science and Technology Programmes } 1 (copy)
Controller, Projects and Analytical Studies
Defence Science Representative (U.K.) (Doc. Data sheet only)
Counsellor, Defence Science (U.S.A.) (Doc. Data sheet only)
Defence Central Library
Document Exchange Centre, D.I.S.B. (17 copies)
Joint Intelligence Organisation
Librarian H Block, Victoria Barracks, Melbourne
Director General—Army Development (NSO) (4 copies)
Defence Industry and Materiel Policy, FAS

Aeronautical Research Laboratories

Director
Library
Superintendent—Aerodynamics
Divisional File—Aerodynamics
Author: D. H. Thompson (4 copies)
D. A. Lemaire
M. J. Williams
K. R. Reddy

Materials Research Laboratories

Director/Library

Defence Research Centre

Library

RAN Research Laboratory

Library

Navy Office

Navy Scientific Adviser

Air Force Office

Air Force Scientific Adviser
Aircraft Research and Development Unit
Library
Technical Division Library
RAAF Academy, Point Cook

DEPARTMENT OF DEFENCE SUPPORT

Government Aircraft Factories
Library

DEPARTMENT OF AVIATION
Library
Flying Operations and Airworthiness Division

STATUTORY AND STATE AUTHORITIES AND INDUSTRY
Commonwealth Aircraft Corporation, Library
Hawker de Havilland Aust. Pty. Ltd., Bankstown, Library

UNIVERSITIES AND COLLEGES

Adelaide	Barr Smith Library
Melbourne	Engineering Library
Monash	Hargrave Library
Newcastle	Library
Sydney	Engineering Library
N.S.W.	Physical Sciences Library
	Professor R. A. A. Bryant, Mechanical Engineering
	Assoc. Professor R. W. Traill-Nash, Civil Engineering
Queensland	Library
Tasmania	Engineering Library
Western Australia	Library
	Associate Professor J. A. Cole, Mechanical Engineering
R.M.I.T.	Library
	Dr H. Kowalski, Mech. & Production Engineering

CANADA
NRC
Aeronautical & Mechanical Engineering Library

Universities and Colleges

Toronto	Institute for Aerospace Studies

FRANCE
ONERA, Library

INDIA
Defence Ministry, Aero Development Establishment, Library

ISRAEL
Technion-Israel Institute of Technology
Professor J. Singer

ITALY
Professor Ing. Guiseppe Gabrielli

JAPAN

Institute of Space and Astronautical Science, Library

NETHERLANDS

National Aerospace Laboratory (NLR), Library

NEW ZEALAND

Universities

Canterbury	Library
	Professor D. Stevenson, Mechanical Engineering

SWEDEN

Aeronautical Research Institute, Library

SWITZERLAND

F+W (Swiss Federal Aircraft Factory)

UNITED KINGDOM

CAARC, Secretary (NRL)
Royal Aircraft Establishment
Bedford, Library
National Physical Laboratory, Library
British Library, Lending Division
Aircraft Research Association, Library
British Ship Research Association
National Maritime Institute, Library
British Aerospace
Kingston-upon-Thames, Library
Hatfield-Chester Division, Library
Westland Helicopters Ltd., Library
Short Brothers Ltd., Technical Library

Universities and Colleges

Bristol	Engineering Library
Cambridge	Library, Engineering Department
London	Professor G. J. Hancock, Aero Engineering
Manchester	Professor N. Johannesen, Fluid Mechanics
Nottingham	Science Library
Southampton	Library
Liverpool	Fluid Mechanics Division, Dr J. C. Gibbings
Strathclyde	Library
Cranfield Institute of Technology	Library
Imperial College	Aeronautics Library

UNITED STATES OF AMERICA

NASA Scientific and Technical Information Facility
Applied Mechanics Reviews
Bell Helicopter Textron, Library
United Technologies Corporation, Library
Lockheed-California Company
Lockheed Missiles and Space Company
Lockheed Georgia
McDonnell Aircraft Company, Library
Analytical Methods Inc., Dr B. Maskew

Universities and Colleges

Johns Hopkins	Professor S. Corrsin, Engineering
Princeton	Professor G. L. Mellor, Mechanics
Massachusetts Inst. of Technology	M.I.T. Libraries
Georgia Institute of Technology	Director, School of Aerospace Engineering

SPARES (10 copies)

TOTAL (121 copies)

Department of Defence Support

DOCUMENT CONTROL DATA

1. a. AR No.	1. b Establishment No.	2. Document Date	3. Task No
AR-002-988	ARL AERO-NOTE-421	November, 1983	DST 82 (

4. Title	5. Security	6. No. Page
A FLOW VISUALISATION STUDY OF TIP VORTEX FORMATION	a. document: Unclassified b. title: U. c. abstract: U.	11 7. No. Refs: 20

8. Author(s)	9. Downgrading Instructions
D. H. Thompson	—

10. Corporate Author and Address	11. Authority (*as appropriate*)
Aeronautical Research Laboratories, G.P.O. Box 4331, Melbourne, Vic. 3001.	a. Sponsor c. Downgradi b. Security d. Approval —

12. Secondary Distribution (*of this document*

Approved for public release.

Overseas enquirers outside stated limitations should be referred through ASDIS, Defence Information Branch, Department of Defence, Campbell Park, CANBERRA, ACT, 2601.

13. a. This document may be ANNOUNCED in catalogues and awareness services available to . . .

No limitations.

13. b. Citation for other purposes (*i.e. casual announcement*) may be (*select*) unrestricted (*or*) as for 13 :

14. Descriptors	15. COSATI G
Flow visualisation	0102
Vortices	0103
Wakes	2004
Wing tips	
Rectangular wings	
Wings	

16. Abstract

The process by which a wing or rotor blade tip vortex is generated has been studied in a tunnel using dye and hydrogen bubble flow visualisation techniques. In particular, the of the shape of the lateral tip edge on vortex formation have been examined. Three edge were tested—a square tip, a square tip with rounded fairing, and a square tip with bevelled f The square tip was found to have the most complicated vortex system, with vortices fo on the tip edge face as well as above the wing. The observed flow features were generally sim those proposed in the literature on the basis of pressure measurements, velocity measure and surface flow visualisation in wind tunnels and on whirl towers. The vortex systems j rounded and bevelled tips were less complicated. The shape of the tip edge has a significant on the structure of the tip vortex system, and may thus influence the tip loading characte Verification of this will require further testing.

This page is to be used to record information which is required by the Establishment for its own use but which will not be added to the DISTIS data base unless specifically requested.

16. Abstract (*Contd*)

17. Imprint

Aeronautical Research Laboratories, Melbourne

18. Document Series and Number	19. Cost Code	20. Type of Report and Period Covered
Aerodynamics Note 421	537700	—

21. Computer Programs Used

—

22. Establishment File Ref(s)

END

FILMED

8